



# LUND UNIVERSITY

## Theoretical and Experimental Study of an Optical Parametric Chirped Pulse Amplification

Zaouter, Yoann

2003

[Link to publication](#)

*Citation for published version (APA):*

Zaouter, Y. (2003). *Theoretical and Experimental Study of an Optical Parametric Chirped Pulse Amplification*. (Lund Reports in Atomic Physics; Vol. LRAP-308). Atomic Physics, Department of Physics, Lund University.

*Total number of authors:*

1

### General rights

Unless other specific re-use rights are stated the following general rights apply:

Copyright and moral rights for the publications made accessible in the public portal are retained by the authors and/or other copyright owners and it is a condition of accessing publications that users recognise and abide by the legal requirements associated with these rights.

- Users may download and print one copy of any publication from the public portal for the purpose of private study or research.
- You may not further distribute the material or use it for any profit-making activity or commercial gain
- You may freely distribute the URL identifying the publication in the public portal

Read more about Creative commons licenses: <https://creativecommons.org/licenses/>

### Take down policy

If you believe that this document breaches copyright please contact us providing details, and we will remove access to the work immediately and investigate your claim.

LUND UNIVERSITY

PO Box 117  
221 00 Lund  
+46 46-222 00 00

**Theoretical and Experimental Studies  
of an Optical Parametric Chirped  
Pulse Amplification**



Report  
by  
Yoann Zaouter

Lund Reports on Atomic Physics, LRAP-308  
Lund, August 2003

To my beloved Karin

# Table of contents

<b><u>ACKNOWLEDGEMENTS</u></b>	<b>3</b>
<b><u>ABSTRACT</u></b>	<b>4</b>
<b><u>INTRODUCTION</u></b>	<b>5</b>
<b><u>1 - THE DIVISION OF ATOMIC PHYSICS</u></b>	<b>5</b>
<b><u>2 - THE LUND LASER CENTRE</u></b>	<b>5</b>
<b><u>3 - CONTEXT OF THE TRAINING PERIOD</u></b>	<b>6</b>
<b><u>4 - PRESENTATION OF THE SUBJECT</u></b>	<b>6</b>
<b><u>PRESENTATION OF THE FIELD OF STUDIES</u></b>	<b>6</b>
<b><u>5 - SUMMARY OF THE DIFFERENT STAGES OF THE STUDY</u></b>	<b>7</b>
<b><u>DESIGN OF THE PARAMETERS OF THE AMPLIFIER</u></b>	<b>9</b>
<b><u>1 - PHASE MATCHING ANGLE AND PHASE MISMATCH IN A COLLINEAR GEOMETRY</u></b>	<b>9</b>
<b><u>PHASE-MATCHING ANGLE</u></b>	<b>10</b>
<b><u>PHASE MISMATCH AS A FUNCTION OF THE SIGNAL WAVELENGTH</u></b>	<b>12</b>
<b><u>CONCLUSION</u></b>	<b>14</b>
<b><u>2 - PHASE MATCHING ANGLE AND PHASE MISMATCH IN A NON-COLLINEAR GEOMETRY</u></b>	<b>15</b>
<b><u>PHASE-MATCHING ANGLE</u></b>	<b>15</b>
<b><u>PHASE MISMATCH AS A FUNCTION OF THE SIGNAL WAVELENGTH</u></b>	<b>17</b>
<b><u>3 - GAIN OF THE AMPLIFIER IN THE NON-COLLINEAR GEOMETRY</u></b>	<b>18</b>
<b><u>4 - DESIGN OF THE PARAMETERS OF THE AMPLIFIER</u></b>	<b>19</b>
<b><u>FIXED AND VARIABLE PARAMETERS</u></b>	<b>20</b>
<b><u>DETERMINATION OF THE BIREFRINGENCE WALK-OFF</u></b>	<b>20</b>
<b><u>OVERLAP IN THE CRYSTAL</u></b>	<b>21</b>
<b><u>DEPLETION OF THE PUMP BEAM</u></b>	<b>23</b>
<b><u>SETUP, MEASUREMENTS AND RESULTS</u></b>	<b>26</b>
<b><u>INTRODUCTION TO THE SETUP</u></b>	<b>26</b>
<b><u>POSITION OF THE BEAMS</u></b>	<b>26</b>
<b><u>SITUATION IN THE LABORATORY</u></b>	<b>26</b>
<b><u>ABOUT THE LASERS</u></b>	<b>27</b>
<b><u>EXPERIMENTAL SETUP</u></b>	<b>28</b>
<b><u>OVERLAPPING OF THE BEAMS INTO THE CRYSTAL</u></b>	<b>28</b>
<b><u>MEASUREMENT OF THE SPECTRAL GAIN</u></b>	<b>31</b>
<b><u>INTRODUCTION TO THE MEASUREMENTS</u></b>	<b>31</b>
<b><u>AMPLIFICATION WITH THE SEEDED PUMP LASER</u></b>	<b>32</b>

---

<u>AMPLIFICATION WITH THE UNSEEDED PUMP LASER</u>	33
<u>COMPRESSION OF THE PULSE</u>	36
<u>INTRODUCTION ABOUT THE COMPRESSION</u>	36
<u>PRISM COMPRESSOR</u>	36
<u>AUTOCORRELATION OF THE PULSE</u>	37
<u>AUTOCORRELATOR MULTI-SHOT</u>	38
<u>AUTOCORRELATOR SINGLE-SHOT</u>	39
<u>DISCUSSION AND CONCLUSION</u>	41
<u>DISCUSSION ABOUT THE EXPERIMENT</u>	41
<u>CONCLUSION ABOUT THIS TRAINING PERIOD</u>	42
<u>LIST AND DESCRIPTION OF THE OPTICAL COMPONENTS</u>	43
<u>REFERENCES</u>	44
<u>ANNEXE I - CALCULATIONS</u>	46
<u>ANNEXE II</u>	60
<u>EXPERIMENTAL SETUP</u>	69
<u>NOTES</u>	70

## Acknowledgements

I would like to warmly thank my supervisors, Anne L'Huiller and Karoly Osvay, for letting me become part of the Atomics Physic Division at LTH in Lund. Thank you to Sophie Kazamias, my supervisor in France, for reading this report and come listen my presentation in Sweden. Those six months changed me and my view of scientific work in more ways than I can explain. Thank you Karoly for being a source of inspiration and energy. What I learned with you is invaluable. This training period and the work I made with you are engraved into my heart. The time I spent here has been a continuous improvement for me as a person and also as a scientist. That is why I owe you my deepest thanks.

I also would like to thank Anders Persson for being always ready to help and without whom nothing would have been possible, Claes-Göran Wahlström for the motivation and the help he gave me.

And of course I owe special thanks to all my colleagues, Diploma workers and PhD students with whom it was a great pleasure to work; Linda Persson, Ann Johansson, Rodrigo Lopez, Filip Lindau, Per Johnsson, Johan Mauritsson, Billy Kaldvee, Magnus Bengtsson, Christopher Abrahamsson, and all the others, Laila Levin, Åke Bergquist, Bertil Hermansson ...

I will always remember those days and nights in my lab, driven by enthusiasm, when suddenly everything works and the adrenaline it gives, but also the football and innebandy games, the parties we have had together talking about everything. And above all I will never forget the sound of the focused ten-hertz Nd:YAG laser ticking on my burning papers and sometimes on my fingers. This "Tack Tack Tack ..." that can drive you crazy if nothing goes right but that makes you feel tremendously happy when you see on the oscilloscope your gain growing and reaching a value that you can not even estimate so it is enormous.

## Abstract

This report summarizes theoretical and experimental work I carried out at the High Intensity Laser Facility at the Lund Laser Centre. The work I am going to explain began at the beginning of March 2003 and ended a few days ago during that month of August 2003. That training period will allow me to complete my fourth year education, out a total of five, at the New Engineer School specialized in Optronics – NFI Optronique – engineering school that is situated on the University Paris XI Orsay campus – France -.

The interest in obtaining high laser intensity in femtosecond or even shorter pulses has never stopped growing in the past few years. Nowadays a new device that exploits the parametric coupling of a high-intensity narrow-band pump pulse and a weak stretched-in-time and broadband signal beam into a non-linear medium gives great hopes to the scientific community for making progress towards higher intensities and shorter laser pulses. My work here consists in studying and setting up this new amplifier known as Optical Parametric Chirped Pulse Amplifier.

My theoretical work allowed me to define several critical parameters for the amplifier. I determined that an angle of phase-matching of 23,8 degrees and an angle of non-collinearity of 2,34 degrees for a BBO crystal cut at 26,1 degrees were the best values for a high and broadband amplification.

The experimental work consisted in setting up a Non-collinear OPCPA that exhibits a minimum gain of 1000. Using a seeded Nd:YAG laser I obtained a stable gain of 500 with a 70 nm bandwidth for a pump intensity of 50 mJ into the crystal. Using 25 mJ from the same Nd:YAG laser but unseeded I achieved a flat gain varying around 9 000 on a very large bandwidth.

The recompression of the amplified stretched-in-time signal pulse and the measurement of the length of the pulse was the last experiment I did. I used a pair of Brewster's prisms, in order to introduce the negative Group Delay Dispersion needed to recompress the pulse. But unfortunately I could not measure the recompressed amplified signal that was totally flooded into the noise of the 80 MHz - non amplified - signal. Nevertheless I manage to recompress the 80 MHz - non amplified - beam from a length of 1 ps to 40 fs.

## Introduction

### 1 - The Division of Atomic Physics

The Division of Atomic Physics of the Lund Institute of Technology (LTH) is responsible for basic physics teaching in all engineering disciplines and for specialised teaching in optics, atomic physics, spectroscopy, laser physics and applications of these disciplines. Research activities at the Division are mainly carried out in the fields of basic and applied spectroscopy, largely based on the use of lasers. The Division of Atomic Physics is also one of nine divisions of the Department of Physics at Lund University.

Research at the Division of Atomic Physics takes place in a multi-disciplinary atmosphere, in which informal collaboration with external scientists and industry takes an important part. The Division is part of the Lund Laser Centre (LLC) which was officially established at Lund University in 1995.

### 2 - The Lund Laser Centre

The purpose of the Centre is to coordinate research and graduate teaching in the fields of lasers, optics, and optical spectroscopy at Lund University and to constitute a base organisation for broad grant applications to the European Community (EC) and other large organisations.

The Lund Laser Centre is formed from parts of several Divisions, which names are:

- Division of Atomic Physics
- Division of Atomic Spectroscopy / Atomic Astrophysics
- Division of Combustion Physics
- Division of Chemical Physics

The Lund University Medical Laser Centre (LUMLC) also is part of the LLC, while two further organisations, the Combustion Centre and the Environmental Measurement Techniques Centre, are associated members.

Following a proposal to the European Community, the LLC was accepted as a European Large Scale Facility with funding for receiving European research group for joint experiments using LLC installations. This programme provides a truly international atmosphere at the Centre, which is characterized by deep specialized knowledge combined with cross-disciplinary activities. Five European Large Scale Facilities are associated in a cluster:



- European Laboratory for Non-Linear Spectroscopy (LENS), Florence, Italy
- Laboratoire d'Optique Appliquée (LOA), Palaiseau, France
- Max-Born Institut (MBI), Berlin, Germany
- FORTH-ULF (Ultra-violet Laser Facility), Heraklion, Greece
- Laser Centre Vrije Universiteit (LCVU), Amsterdam, The Netherlands

### **3 - Context of the training period**

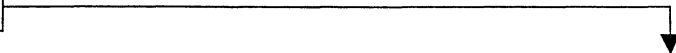
This six-month training is part of my fourth year education at the NFI Optronique school of the University of Paris Sud – Orsay. After a first training period as a worker within Georg Fisher Disa (Palaiseau – France) and two training as a higher technician level within Thales Optronique (Guillancourt –France) and the Institut de Radioprotection et de Sûreté Nucléaire (IRSN – Fontenay-aux-Roses – France) this fourth training period of a longer length than the previous ones will allow me to achieve my fourth year education out a total of five.

I applied for a training period at the Lund Laser Centre because I wanted to reach a new level in my education. After two three-month training periods in France where I worked on optical systems (military thermal cameras) and electronics (acquisition card of a neutron detector), I wanted to work in a laser environment, and especially with high power lasers. This new training period was also ideal to put in application new knowledge learned in the fourth year such as laser and non-linear optics. Furthermore I also wanted to work abroad in order to improve my level in English.

Hence this training period within the Atomic Physics Department of the Lund Laser Centre followed exactly my wishes and it was a great opportunity to work in Lund in this world-known laboratory.

### **4 - Presentation of the subject**

Presentation of the field of studies



The appearance of chirped pulse amplification (CPA) was a major breakthrough for high-power short-pulse lasers

. This method includes four stages:

- 1) A weak ultra-short pulse is generated ( $<5$  nJ,  $\approx 15$  fs)
- 2) It is stretched in time (up to 500 ps)
- 3) then it is amplified (up to few Joules)
- 4) and finally compressed in time (down to 15-20fs)

This CPA technique has been first implemented in Nd:glass laser facilities and has recently enable the production of pulses with power around 1 PW and focused intensity that exceeds  $10^{21}$  W/cm<sup>2</sup> on target.

But the Nd:glass medium has several drawbacks among which a process known as gain narrowing limits the pulse bandwidth to 1 nm (although Nd:glass has a large fluorescence bandwidth of approximately 20 nm) and thus a shortest pulse duration to about 1 ps due to.

The Titanium sapphire medium has an interesting broad amplification bandwidth lying from 690 to 1080 nm. However, the single-pass gain is modest. This Ti:sapphire amplification medium is often used in a regenerative cavity system where there is typically 70 to 100 round trips. However this scheme still suffers from gain narrowing and poor temporal contrast due to low-level pre-pulses and a high level of spontaneous emission amplification that originates from polarisation optics and the multi-pass nature of the system.

Following the ideas originally proposed by Dubietis *et al.*<sup>(1)</sup>, a new amplification technique for ultra-short pulses was presented in detail in a theoretical paper by Ross *et al.*<sup>(2)</sup>. This new amplification technique that offers exciting prospects for generating new extremes in power, in intensity and also in pulse duration is known as Optical Parametric Chirped Pulse Amplification (OPCPA)<sup>(3)-(8)</sup>.

With the use of parametric coupling of a high-energy pump field and a low-energy broadband and stretched-in-time signal field in a non-linear crystal, the OPCPA technique is able to offer extremely high and spectrally flat gain, in single-pass amplification, simultaneously with extremely large bandwidths and a low level of gain narrowing. This technique has also some really appreciable advantages, which will be considered later in this report, in comparison with other amplification techniques.

## **5 - Summary of the different stages of the study**

My work on the OPCPA scheme could be divided into four stages that has taken more or less time. In the first part of my work in Lund, I did calculations about the different critical parameters of the amplifier after having read several articles and/or books dealing with non-linear process in uniaxial crystals and (N)OPCPA. This took couple of months.

During the second period, I set up the experiment directing the laser beams into my laboratory and setting up optical pathways in order to get a satisfying amplification. In the third part, I did the measurements and characterisation of the amplifier. Those two experimental parts required almost 4 months.

The remaining time was dedicated to the writing of this report and the preparation of a presentation for the Atomic Physics Division.

## Design of the Parameters of the Amplifier

### 1 - Phase matching angle and phase mismatch in a collinear geometry

In the process of optical parametric chirped pulse amplification, a chirped signal pulse ( $E_s$ ) is amplified through optical parametric amplification. The energy of a narrow-band pump pulse ( $E_p$ ) is transferred to the signal pulse through direct coupling of these two fields in a non-linear optical crystal. To conserve photon energy and momentum, a third field called “idler” ( $E_i$ ) is created during the amplification. Simultaneously, the signal beam is coherently amplified. This is formally described by a system of coupled differential equations for the amplitudes of the three waves, which was derived by Armstrong *et al*<sup>(9)</sup>.

$$\left\{ \begin{array}{l} \frac{d E_s}{d z} = i \cdot \frac{2\omega_s}{n_s c} \cdot d_{\text{eff}} E_i^* \cdot E_p \cdot \exp(i \Delta k \cdot z) \\ \frac{d E_i}{d z} = i \cdot \frac{2\omega_i}{n_i c} \cdot d_{\text{eff}} E_s^* \cdot E_p \cdot \exp(i \Delta k \cdot z) \\ \frac{d E_p}{d z} = i \cdot \frac{2\omega_p}{n_p c} \cdot d_{\text{eff}} E_s \cdot E_i \cdot \exp(-i \Delta k \cdot z) \end{array} \right.$$

Where  $z$  is the coordinate in the propagation direction,  $d_{\text{eff}}$  is the effective non-linearity of the medium,  $n_p$ ,  $n_s$ ,  $n_i$ , are the indexes of the pump, signal and idler beams and  $\Delta k$  is the phase mismatch.

To transfer the energy from the pump pulse to the signal pulse with a maximum efficiency, all the frequencies must propagate through the crystal at equal (phase) velocity. This condition is known as the **phase-matching** condition. It would normally never occur except by considering the birefringence that exhibits most of the crystals. Thus it is possible to achieve this phase-matching condition by choosing appropriate polarizations and propagation directions.

The first task I had to perform was to define the angle of phase-matching i.e. the angle  $\theta$  with respect to the optical axis (Z-axis) of the crystal that makes possible to close the k-vector triangle and thus achieve the phase matching condition.

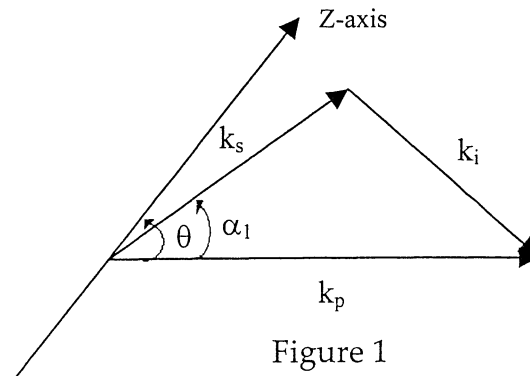


Figure 1

In Figure 1  $\vec{k}_p$ ,  $\vec{k}_s$ ,  $\vec{k}_i$  are respectively the k-vector of the pump, signal and idler beams.

From the k-vector triangle, we obtain a first equation for the collinear case (i.e.  $\alpha_1 = 0$ ) that can be written:

$$\begin{aligned} \vec{k}_p = \vec{k}_s + \vec{k}_i &\Leftrightarrow \frac{2\pi \cdot n_p}{\lambda_p} = \frac{2\pi \cdot n_s}{\lambda_s} + \frac{2\pi \cdot n_i}{\lambda_i} \\ &\Leftrightarrow \frac{n_p}{\lambda_p} = \frac{n_s}{\lambda_s} + \frac{n_i}{\lambda_i} \end{aligned} \quad (1)$$

Where  $n_p$ ,  $n_s$ , and  $n_i$  are respectively the indices of the pump, signal and idler beams.

However  $n_p$ , the index of the pump beam, is a function of  $\theta$  the angle of phase-matching. For propagation at an angle  $\theta$  with respect to the Z-axis, the index of the wave is given by:

$$\frac{1}{[n(\theta)]^2} = \frac{\cos^2(\theta)}{[n^o]^2} + \frac{\sin^2(\theta)}{[n^e]^2} \quad (2)$$

Where  $n^o$  and  $n^e$  stand for the index of the wave on the principal axes of the crystal, “o” stand for Ordinary and “e” for Extraordinary.

Phase-Matching angle



Using equations (1) and (2), it is possible to determine the phase-matching condition, with the help of MathCad.

First we have to determine the wavelength of the idler wave for a pump beam and a signal beam that have wavelengths of 532 nm and 800 nm. Following the principle of energy conservation,

$$\omega_p = \omega_s + \omega_i \quad \Rightarrow \quad \frac{1}{\lambda_i} = \frac{1}{\lambda_p} - \frac{1}{\lambda_s}$$

The associated MathCad syntax is given,

<b>Energy conservation:</b>	
Wavelengths:	$\lambda_p := 0.532$
	$\lambda_s := 0.800$
	$\lambda_i := (\lambda_p^{-1} - \lambda_s^{-1})^{-1}$
	$\lambda_i = 1.588$

In a second time, we have to determine the different indices of the signal and idler beams on the ordinary axis and of the pump beam on the ordinary and extraordinary axes. To perform this task we use the Sellmeier equation:

$$\begin{cases} n^{o^2}(\lambda) = 2,7359 + \left( \frac{0,01878}{\lambda^2 - 0,01822} \right) - 0,01354 \cdot \lambda^2 \\ n^{e^2}(\lambda) = 2,3753 + \left( \frac{0,01224}{\lambda^2 - 0,01667} \right) - 0,01516 \cdot \lambda^2 \end{cases} \quad (\lambda \text{ in } \mu\text{m})$$

The MathCad syntax is given below:

<b>Refractive Index: Sellmeier Equation:</b>	
$n_{po} := \sqrt{2.7359 + \left( \frac{0.01878}{\lambda_p^2 - 0.01822} \right) - 0.01354 \lambda_p^2}$	$n_{po} = 1.674$
$n_{pe} := \sqrt{2.3753 + \left( \frac{0.01224}{\lambda_p^2 - 0.01667} \right) - 0.01516 \lambda_p^2}$	$n_{pe} = 1.555$
$n_{so} := \sqrt{2.7359 + \left( \frac{0.01878}{\lambda_s^2 - 0.01822} \right) - 0.01354 \lambda_s^2}$	$n_{so} = 1.661$
$n_{io} := \sqrt{2.7359 + \left( \frac{0.01878}{\lambda_i^2 - 0.01822} \right) - 0.01354 \lambda_i^2}$	$n_{io} = 1.646$

*n<sub>po</sub> and n<sub>pe</sub> are the indices of the pump beam for the ordinary and extraordinary axes while n<sub>so</sub> and n<sub>io</sub> are the indices of the signal and idler beams for the ordinary axis.*

Remark

It is now possible to determine the phase-matching angle using a typical MathCad syntax given below:

**Determination of the Phase-Matching Angle  $\theta$ :**

$$n_p(\theta) := \sqrt{\left( \frac{\cos(\theta)^2}{n_{po}^2} + \frac{\sin(\theta)^2}{n_{pe}^2} \right)^{-1}}$$

$\theta\theta := 21 \text{ deg}$

Given

$$\frac{n_p(\theta\theta)}{\lambda_p} = \frac{n_{so}}{\lambda_s} + \frac{n_{io}}{\lambda_i}$$

$\theta_c := \text{Find}(\theta\theta)$

$\theta_c = 22.056 \text{ deg}$

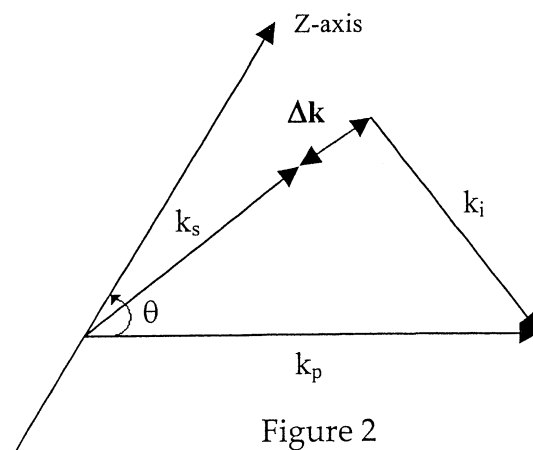
$n_p(\theta_c) = 1.6529$

Thus the phase-matching angle for this collinear geometry slightly exceeds 22 degrees and the index of the pump wave in the crystal is 1,6529. Furthermore the angle of phase-matching has to be strongly respected if we want to achieve a maximum transfer of the energy from the pump to the signal beam.

Phase Mismatch as a function of the signal wavelength

The next step of the study of this collinear geometry of our OPCPA is to determine the behaviour of the phase mismatch for a signal wavelength varying between 750 and 850 nm.

The phase-mismatch occurs when we cannot close the k-vector triangle as shown in figure 2 below:



Hence we can determine the Phase Mismatch from:

$$\Delta \vec{k} = \vec{k}_p - \vec{k}_s - \vec{k}_i \quad (3)$$

To draw the graph of the phase mismatch as a function of the signal wavelength, we have to proceed in three different stages in MathCad. First it is necessary to define several functions such as the wavelength of the idler, the indices of the signal and the idler beams, and the phase mismatch as a function of the signal wavelength. Next we have to represent the signal wavelength and the phase mismatch as vectors (see bellow) in order to draw the evolution of the phase mismatch in a third stage. We can see underneath the result of the programming of those three stages:

**Phase-Matching as a function of the Wavelength:**

**Functions and Variables:**

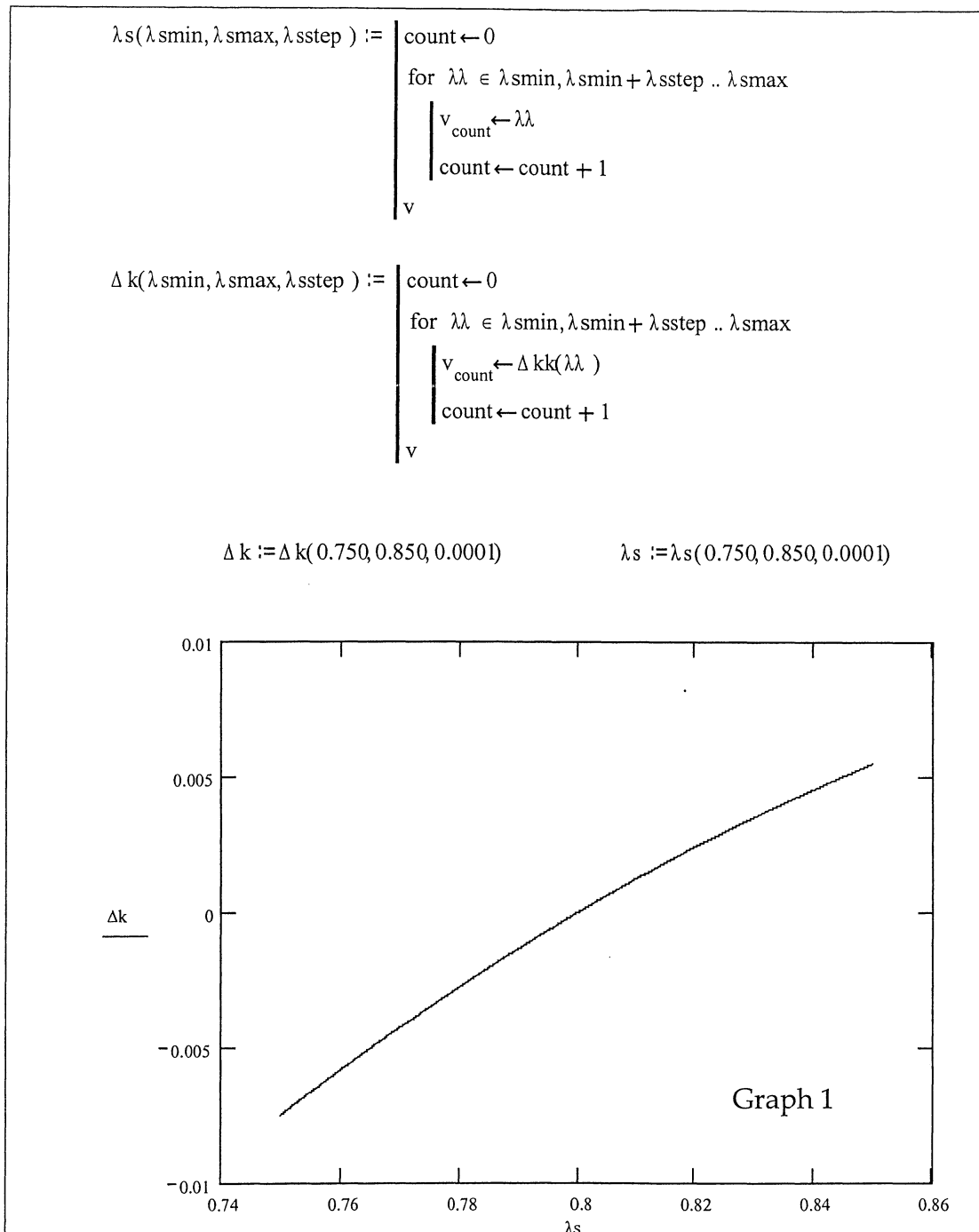
$$\lambda_i(\lambda) := (\lambda_p^{-1} - \lambda^{-1})^{-1}$$

$$n_s(\lambda) := \sqrt{2.7359 + \left( \frac{0.01878}{\lambda^2 - 0.01822} \right) - 0.01354\lambda^2}$$

$$n_i(\lambda) := \sqrt{2.7359 + \left( \frac{0.01878}{(\lambda_i(\lambda))^2 - 0.01822} \right) - 0.01354\lambda_i(\lambda)^2}$$

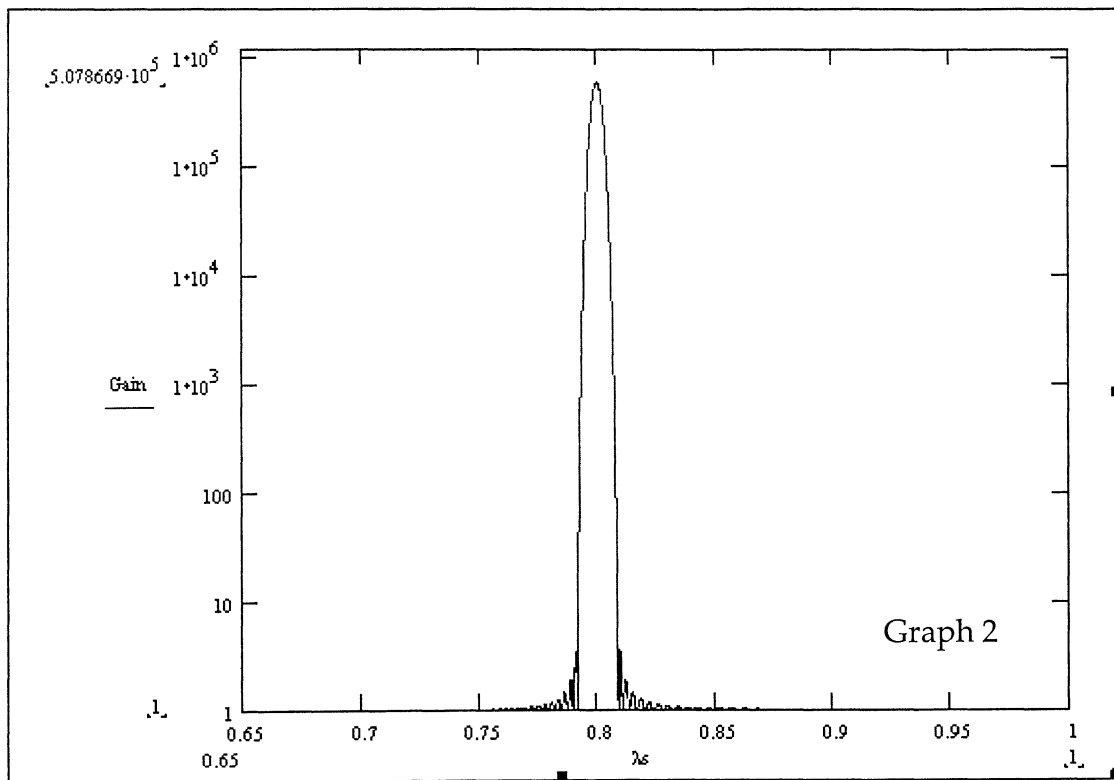
$$\Delta k(\lambda) := \frac{2\pi \cdot n_p(\theta_c)}{\lambda_p} - \frac{2\pi \cdot n_s(\lambda)}{\lambda} - \frac{2\pi \cdot n_i(\lambda)}{\lambda_i(\lambda)}$$





**Conclusion**

We show the evolution of the phase mismatch for a phase-matching that optimizes the amplification for a signal wavelength of 800 nm in Graph 1. This graph shows how the phase mismatch is important in the vicinity of 800 nm. The amplification will be satisfactory only in a very small area around the central wavelength of the signal as represented in the Graph 2 besides:



$$\max(\text{Gain}) = 5.079 \cdot 10^5$$

$$\text{Gain}_{2000} = 5.079 \cdot 10^5$$

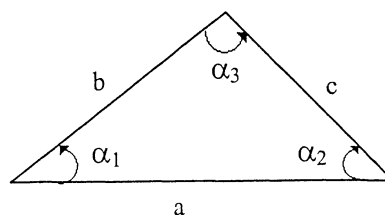
So it is necessary to introduce a new parameter to reveal the potential gain bandwidth of this amplifier. Thus we introduce a slight non-collinearity between the pump and signal beams.

## 2 - Phase matching angle and phase mismatch in a non-collinear geometry

Phase-Matching angle

In the k-vector triangle (Figure 1)  $\alpha_1$  is no longer equal to zero any longer and have to be introduced in the phase-matching equation.

We introduce  $\alpha_1$  and the other angles of the k-vector triangle by the use of “cosinus law” in a triangle:



$$a^2 = b^2 + c^2 - 2.b.c.\cos(\alpha_3) \Leftrightarrow a^2 = b^2 + c^2 - 2.b.c.\cos(\pi/2 - (\alpha_1 + \alpha_2))$$

$$\Leftrightarrow a^2 = b^2 + c^2 + 2.b.c.\cos(\alpha_1 + \alpha_2)$$

The phase-matching equation:  $\bar{k}_p = \bar{k}_s + \bar{k}_i$

$$k_p^2 = k_s^2 + k_i^2 + 2.k_s.k_i.\cos(\alpha_1 + \alpha_2)$$

Futhermore,  $\cos(\alpha_1 + \alpha_2) = \cos(\alpha_1).\cos(\alpha_2) - \sin(\alpha_1).\sin(\alpha_2)$

And,  $k_s.\sin(\alpha_1) = k_i.\sin(\alpha_2)$

The phase-matching equation, as a function of the non-collinear angle  $\alpha_1$ , becomes:

$$k_p^2 = k_s^2 + k_i^2 + 2.k_s.k_i \left[ \sqrt{\left(1 - \frac{k_s}{k_i}.\sin(\alpha_1)\right)^2} \cdot \cos(\alpha_1) - \frac{k_s}{k_i}.\sin^2(\alpha_1) \right] \quad (4)$$

Hence finally,

$$n_p = \sqrt{\lambda_p^2 \left[ \frac{n_i^{\circ 2}}{\lambda_i^2} + \frac{n_s^{\circ 2}}{\lambda_s^2} + 2 \cdot \frac{n_i^{\circ 2} \cdot n_s^{\circ 2}}{\lambda_i \cdot \lambda_s} \left[ \sqrt{\left(1 - \frac{n_s^{\circ}}{n_i^{\circ}} \cdot \frac{\lambda_i}{\lambda_s} \cdot \sin(\alpha_1)\right)^2} \cdot \cos(\alpha_1) - \frac{n_s^{\circ}}{n_i^{\circ}} \cdot \frac{\lambda_i}{\lambda_s} \cdot \sin^2(\alpha_1) \right] \right]} \quad (5)$$

With this last equation and equation (2), which is still valid even in the non-collinear geometry, we can find the phase-matching angle for a fixed value of the angle of non-collinearity  $\alpha_1$ , via the MathCad syntax given above:

**Determination of the Phase-Matching Angle :**

$$np(\theta) := \sqrt{\left(\frac{\cos(\theta)^2}{npo^2} + \frac{\sin(\theta)^2}{npe^2}\right)^{-1}}$$

$\theta\theta := 21 \text{ deg}$   
 $\alpha 1 := 2.34 \text{ deg}$

Given

$$np(\theta\theta) = \sqrt{\lambda_p^2 \left[ \frac{nio^2}{\lambda_i^2} + \frac{nso^2}{\lambda_s^2} + \frac{2 \cdot nio \cdot nso}{\lambda_i \cdot \lambda_s} \left[ \sqrt{\left(1 - \frac{nso \cdot \lambda_i}{nio \cdot \lambda_s} \cdot \sin(\alpha 1)\right)^2} \cdot \cos(\alpha 1) - \frac{nso \cdot \lambda_i}{nio \cdot \lambda_s} \cdot \sin(\alpha 1)^2 \right] \right]}$$

$\theta c := \text{Find}(\theta\theta)$

$\theta c = 23.771 \text{ deg} \quad np(\theta c) = 1.653$

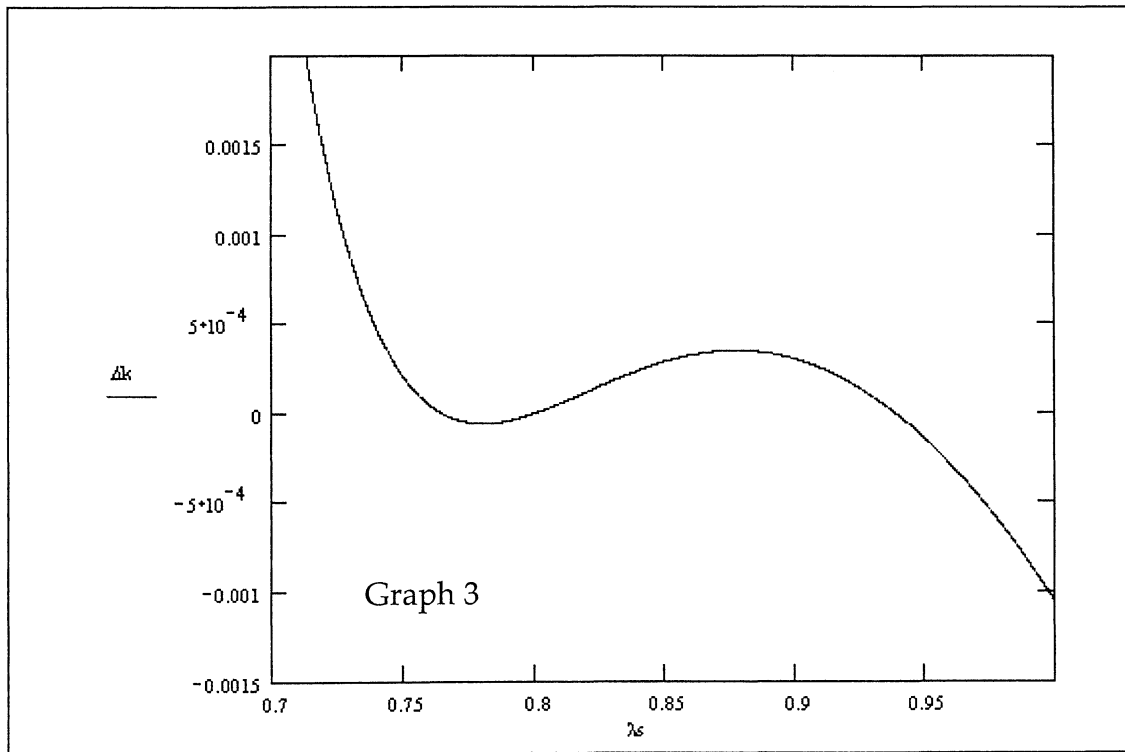
For a given angle of non-collinearity of 2.34 degrees, we obtain a phase-matching angle of  $23.771^\circ$  and an index in the crystal for the pump beam equal to 1.653.

*We will see later that the angle of non-collinearity equal to  $2.34^\circ$  seems to give the broadest amplification bandwidth for our configuration, and that the gain is very sensitive to the value of this angle.*

Remark

Phase Mismatch as a function of the signal wavelength

For this given value of the non-collinearity angle, the shape of the phase mismatch is drawn below:



A basic comparison between Graph 1 and Graph 3 shows that the phase mismatch is appreciably weaker for a non-collinear geometry over a much larger spectral band. This geometry will be more favorable to a broadband amplification.

### 3 – Gain of the amplifier in the Non-Collinear Geometry

We have shown above that the phase mismatch is far smaller over a broader spectral bandwidth in the non-collinear geometry configuration. We now discuss its influence on the gain of the amplifier in terms of peak value and of broadband amplification.

The formula describing the amplification in an OPCPA is given by:

$$\frac{P_s(L)}{P_s(0)} = 1 + (g.L)^2 \frac{\sinh^2(\sqrt{(g.L)^2 - (\Delta k.L/2)^2})}{(g.L)^2 - (\Delta k.L/2)^2} \quad (6)$$

Where the gain coefficient  $g$  is given by:

$$g = 4\pi \cdot d_{\text{eff}} \cdot \sqrt{\frac{I_p(0)}{2\epsilon_0 \cdot n_p \cdot n_s \cdot n_i \cdot c \cdot \lambda_s \cdot \lambda_i}} \quad (7)$$

In equations (6) and (7),  $L$  represents the length of the crystal,  $\Delta k$  is the phase mismatch and  $d_{\text{eff}}$  is the non-linear coefficient that has been contracted from a tensor to a scalar quantity, which is more convenient.

$$d_{\text{eff}} = d_{31} \cdot \sin(\theta) - d_{22} \cdot \cos(\theta) \cdot \sin(3\phi) \quad \text{with } \phi = \pi/2$$

$$d_{31} = 0.16 \text{ pm/V}$$

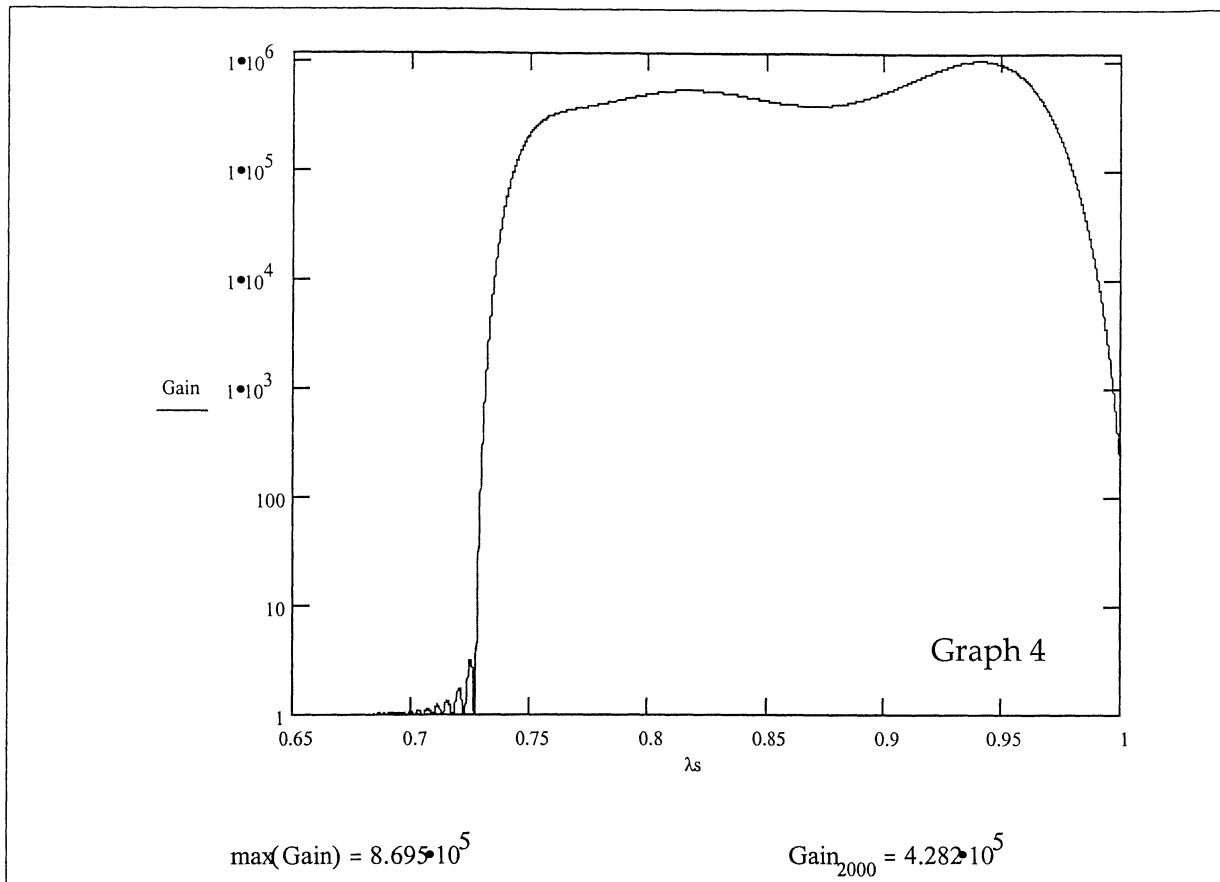
$$d_{22} = 2.3 \text{ pm/V}$$

and  $\theta$  is the phase-matching angle

*This expression of the effective non-linearity  $d_{\text{eff}}$  in the phase-matching direction is given for a BBO crystal ( $\beta\text{-BaB}_2\text{O}_4$ ) for well-defined polarisation directions of the interacting beams. In this specific case  $d_{\text{eff}} = d_{\text{ooe}}$ .*

Remark

The MathCad's syntax is given in Annexe 1 and the gain of the amplifier for a signal wavelength varying between 0.65 and 1  $\mu\text{m}$  is shown below:



*Graph 4 has been plotted for an angle of non-collinearity of 2,34 degrees that seems to be the optimum angle value. The evolution of the phase-mismatch and the gain curve for an angle of non-collinearity varying between 0 and 3 degrees is shown in Annexe 2.*

Remark

#### 4 – Design of the parameters of the amplifier

After this theoretical study and calculation of the non-collinearity and phase matching angles as well as the amplifier gain, it is important to design the different parameters of the amplifier such as:

- pump intensity
- signal intensity
- beam parameters in the crystal (diameters, focal spot etc...)
- and take into account the effect of pump depletion.

We must consider the effects of the birefringence walk-off on the spatial overlapping of the signal and pump beams. It is also important to confirm that we won't exceed the damage threshold of the BBO crystal.

### Fixed and Variable Parameters

#### Pump Beam:

- $\tau \in [6 ; 8 \text{ ns}]$  or at least must be lower than 12 ns
- Energy = Variable
- Diameter = Variable

#### Signal Beam:

- Energy : 4 nJ / pulse
- $\tau_0 = 30 \text{ fs}$  (Transform limited value)
- $\tau \cong 1.2 \text{ ps}$  and at least  $\in [1 ; 5 \text{ ps}]$  (is the FWHM after the stretcher)
- Diameter of 1 mm that can be slightly modified

#### Damage threshold of BBO crystal:

- @ 532 nm :  $< 4.8 \text{ GW.cm}^{-2}$

### Determination of the birefringence walk-off

The effect of walk-off occurs in birefringent media such as BBO crystal. In those media the direction of wave propagation is usually not the same as the direction of energy propagation that follows the Poynting vector given in equation (8)

$$\vec{S} = \frac{1}{\mu_0} \vec{E} \times \vec{B} \quad (8)$$

Hence the ordinary and extraordinary beams won't overlap over the full length of the birefringent media used and the extraordinary beam is seen to "walk-off" the axis of the ordinary beam. For uniaxial crystal such as BBO, the walk-off angle  $\rho$  is given by:

$$\tan(\rho) = \frac{[n^e(\theta)]^2}{2} \left[ \frac{1}{(n^e)^2} - \frac{1}{(n^o)^2} \right] \sin(2\theta) \quad (9)$$

After a Taylor expansion, for a negative crystal, it can be written as:

$$\rho = +\arctan\left[\left(\frac{n^o}{n^e}\right)^2 \cdot \tan(\theta)\right] - \theta \quad (10)$$

The numerical application has been done on MathCad, and can be seen in Annex 1. The walk-off angle  $\rho$  is equal to 3.287 degrees. This means that the real angle between the direction of energy flow of the pump and the signal beam is equal to 0.947 degree.

### Overlap in the crystal

In this non-collinear geometry, it is obvious that the size of the pump beam and the signal beam must not be the same. The pump beam must be larger than the signal one, so both beams will interact through the whole crystal despite the angle between the two beams. We will vary the diameter of the pump beam, to achieve the best spatial overlap of the two beams through the full length of the BBO crystal.

We impose to our amplifier that the signal beam must stay between the 100% and 80% intensity area of the pump beam. So first it is important to calculate the deviation of the signal beam with respect to the pump beam.

Supposing that the deviation is equal to zero at the centre of the crystal:

$$l = \frac{L}{2} \cdot [\tan(\theta - \theta_c + \rho) - \tan(\theta - \theta_c + \alpha)]$$

Where:

- $\theta$  is the angle between the horizontal axis and the Z-axis of the crystal
- $\theta_c$  is the angle of phase-matching i.e. between the pump beam and the Z-axis of the crystal
- $\rho$  is the walk-off angle
- $\alpha$  is the angle of non-collinearity

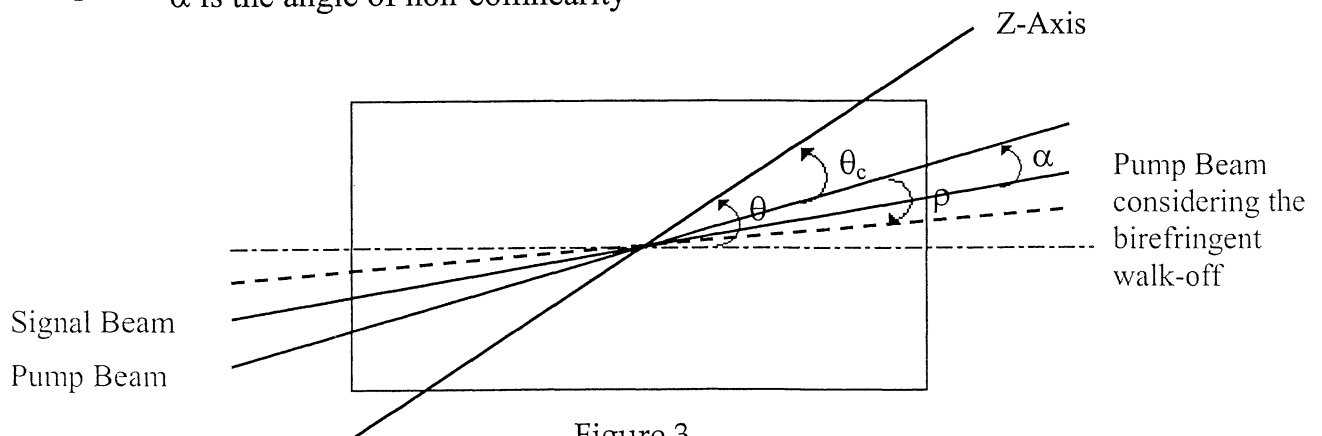


Figure 3

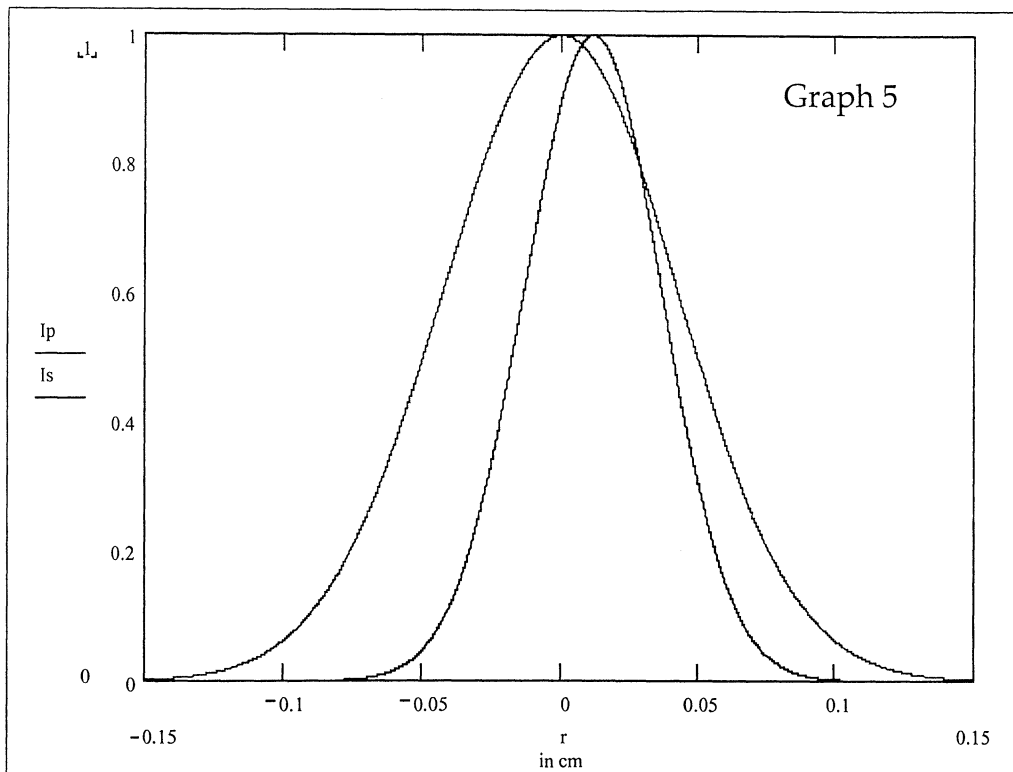


The numerical application made with MathCad gives us a deviation between the signal beam and the pump beam of 116  $\mu\text{m}$  in the front and at the end of the 14 mm crystal. Considering that the spatial shapes of the pump and signal beam are Gaussians, we can determine the diameter of the pump beam so that the signal beam stays between the 100% and 80% intensity area of the pump beam.

The intensity of the pump ( $I_p$ ) and signal beam ( $I_s$ ) can be written as:

$$I_p(r) = I_p \cdot \exp\left[\frac{-2 \cdot r^2}{w_p^2}\right] \qquad I_s(r) = I_s \cdot \exp\left[\frac{-2 \cdot (r+1)^2}{w_s^2}\right]$$

With  $w_s$ , the waist of the signal beam, set to 0.5 mm i.e. a diameter of 1 mm and  $w_p$ , the waist of the pump beam, that has to be determined. We find that the signal beam stays between the 100% and 80% intensity area of the pump beam for  $w_p = 0.85$  mm i.e. a diameter of 1.7 mm. With this value we can draw the position of the signal beam in comparison to the pump beam at the output of the crystal (Graph 4) and we can see that it is inside the “good” intensity area.



Other optimisations of  $w_p$  have been made for different values of  $w_s$  and intensity area in which the signal beam must stay. The results of those calculations are shown in table 1:

	100 - 80 %	100 - 90 %	100 - 95 %
<b><math>w_s = 0.5</math> mm</b>	$w_p = 0.85$ mm	$w_p = 1$ mm	$w_p = 1.23$ mm
<b><math>w_s = 0.375</math> mm</b>	$w_p = 0.725$ mm	$w_p = 0.875$ mm	$w_p = 1.1$ mm
<b><math>w_s = 0.125</math> mm</b>	$w_p = 0.475$ mm	$w_p = 0.68$ mm	$w_p = 0.9$ mm

Table 1

Depletion of the Pump Beam

The last part of this theoretical study of the amplifier has been to investigate the depletion phenomenon that occurs during the amplification. This phenomenon is linked to the transfer of energy from the pump field to the signal field due to the parametric coupling in the crystal. The depletion stayed below a value of 1% considering the pump intensity chosen to achieve a gain of 10 000 (i.e. 545 MW/cm<sup>2</sup> or a fluence of 3,27 J/cm<sup>2</sup>).

To do that, I had to calculate the energy of the pump field and of the signal field after a theoretical gain of 10 000 were calculated. This calculation was performed for two different shapes of the pump beam: Gaussian and top-hat.

Gaussian Profile:

The pump intensity is determined by:

$$I_{\text{pump}} = 2 \int_0^{\infty} \int_0^{\infty} I_{\text{peak}} e^{-2 \frac{(x+y)^2}{W_{\text{pump}}^2}} .dx.dy$$

Its energy is,

$$E_{\text{pump}} = \int_{-\infty}^{\infty} I_{\text{peak}} \exp\left(-4 \ln 2 \left(\frac{t}{\tau}\right)^2\right) dt \approx I_{\text{peak}} \tau$$

Where  $\tau$  is the full width half maximum (FWHM) of the temporal profile.

Assuming a peak intensity of 545 MW/cm<sup>2</sup> (i.e. a gain of 10 000) with a FWHM of 6 ns for the pump beam and an energy of 4nJ for the signal beam, the calculation leads to a total depletion of less than 0.4 %.

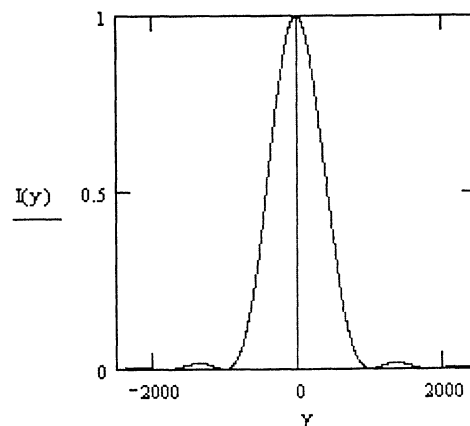
Top-Hat Profile:

The calculation is trickier since we have to consider the spatial distribution of intensity in the diffraction pattern. This can be written in a form known as the Airy formula:

$$I = I_{\text{peak}} \left[ \frac{2J_1(u)}{u} \right]^2$$

Where,

$$\lim_{u \rightarrow 0} \left[ \frac{2J_1(u)}{u} \right] = 1$$



$$u = \frac{k.a.\rho}{2.f} = \frac{\pi.a.\rho}{\lambda.f}$$

where: - k is the wave vector.

- a and f are respectively the aperture and the focal length of the optical system.
- $\rho$  is the radius of the airy disk

First the values of  $f$  and  $a$  were optimized to get a FWHM of the airy disk as close as possible to the value determined previously (cf Table 1). Then it was possible to calculate the energy of the pump using the following equations that give respectively the energy content of the diffraction pattern within a radius of  $\rho$  and the total energy in the Airy disc for a given fluence  $I_0$ :

$$E(\rho) = 2 \int_0^{\frac{\pi \cdot a \cdot \rho}{\lambda_p \cdot f}} \left[ \frac{J_1(x)}{x} \right]^2 dx$$

And,

$$E_{\text{total}} = E\left(\frac{0.61 \cdot \lambda_p \cdot f}{a}\right) \cdot \frac{\lambda_p^2 \cdot f^2}{\pi \cdot a^2} \cdot I_0$$

Finally considering a fluence of  $3.27 \text{ J/cm}^2$  (i.e. a gain of 10 000), the values of  $f$  and  $a$  found to have a waist of the pump beam equal to 0.85 mm (i.e.  $f = 7700 \text{ mm}$  and  $a = 2.5 \text{ mm}$ ) and an energy of 4nJ for the signal beam, the calculation gives a total depletion of less than 0.2 %.

Conclusion about the depletion of the pump beam:

The depletion of the pump beam depletion stays negligible (i.e. lower than 1%) for both types of profile, Gaussian or Top-Hat.

## Setup, Measurements and Results

### Introduction to the Setup

#### Position of the Beams

According to the calculations made for a crystal cut at 26,1degrees and explained in the first part of this report, both beams must interact into the non-linear crystal with an angle of non-collinearity of 2,34 degrees. Considering the birefringence walk-off angle of 3,287 degrees that makes the pump beam move away from the Z-axis of the crystal, we can determine the angle outside the crystal:

- Angle of the pump beam outside the crystal:  $\alpha_p = 3,623$  degrees
- Angle of the signal beam outside the crystal:  $\alpha_s = - 0,018$  degree

Those two angles are measured from the horizontal axis that crosses the crystal in its middle as represented on Figure 4:

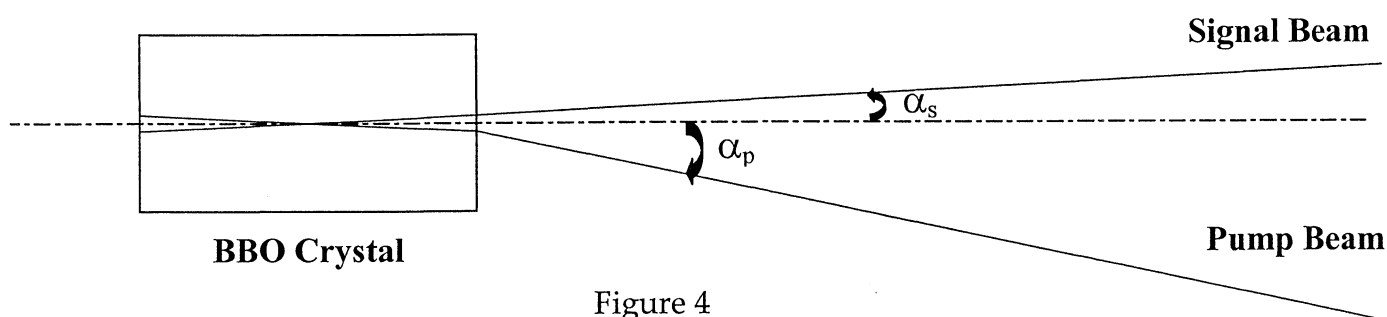


Figure 4

#### Situation in the Laboratory

Physically the two lasers used were not installed in the room where the experiment was performed. The signal beam was coming from the TeraWatt-Lab and had to travel about 30 meters before coming into the experiment room. The pump laser was installed in the VUV-Lab and had to travel over a length of 15 meters before being focused into the crystal.

We will see later that the installation of the lasers plays an important role in the quality of the results. In fact both beams, especially the signal beam, were constantly moving. The intensity of this beam was varying quite much because of the long travel not piped that it had to cover before coming into my experiment room. It was also moving spatially all along the day. At the output of the laser, that movement could completely be neglected but The signal beam had to travel several meters in air leading to fluctuations of intensity. In addition, it lacked pointing stability. After 30 meters the laser could move up to 0,3 mm from its initial position.

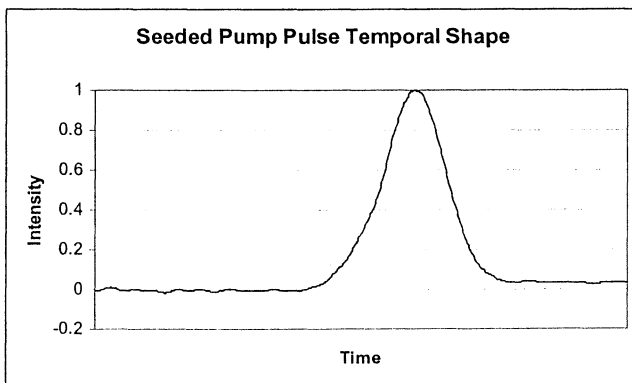
These motions and fluctuations, and to a less extent the fluctuations of the pump beam made the experiment much more unstable that it was expected to be.

### About the Lasers

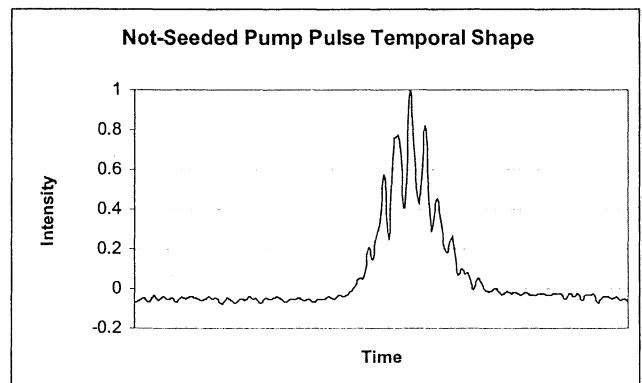
#### - The Pump Laser:

The pump laser was a ten-Hertz and frequency doubled Nd:YAG laser (i.e. 532 nm) that can give an output energy of 700 mJ/pulse over a diameter of 1 cm and a pulse duration of 12 ns. It could be turned on in two different modes: seeded or not.

The temporal shape of the seeded and the unseeded pump laser are given below for an energy of 200 mJ/pulse and a duration of about 6 ns.



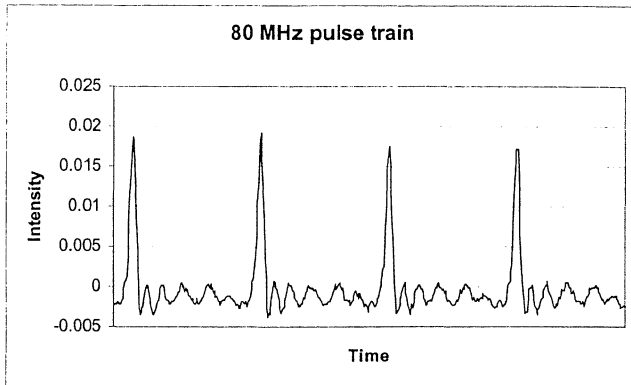
Graph 6



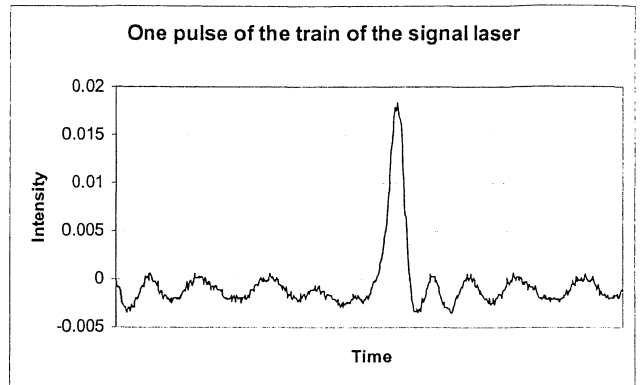
Graph 7

#### - The Signal Laser:

The signal beam is generated by a 80MHz repetition rate Ti:S femtosecond oscillator (from KMLab) pumped by 5W all-line Argon ion laser. The energy of a single pulse is about 4 nJ/pulse over a size of 1 mm. The transform limited duration is around 30 fs, which is stretched up to 1 ps in a “Dazzler” and other optics along the image relay line. The output of this oscillator is represented bellow:



Graph 8



Graph 9

*The width of those pulses is about 1 ns but it is just because the response time of the photodiode used to measure those pulse was 1 ns Their pulse duration is in reality equal to 1 ps.*

Remark

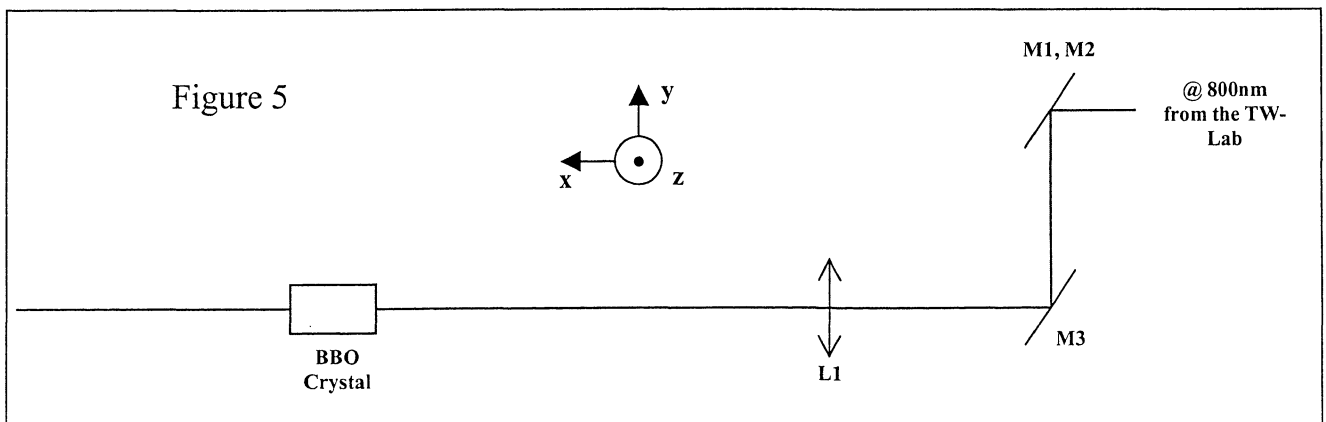
### Experimental Setup

#### Overlapping of the beams into the Crystal

*In the following parts of this report will be introduced several optical components such as mirrors, lenses, wedge plates etc... They are drescribed in more details in the "List ans Description of Optical components"*

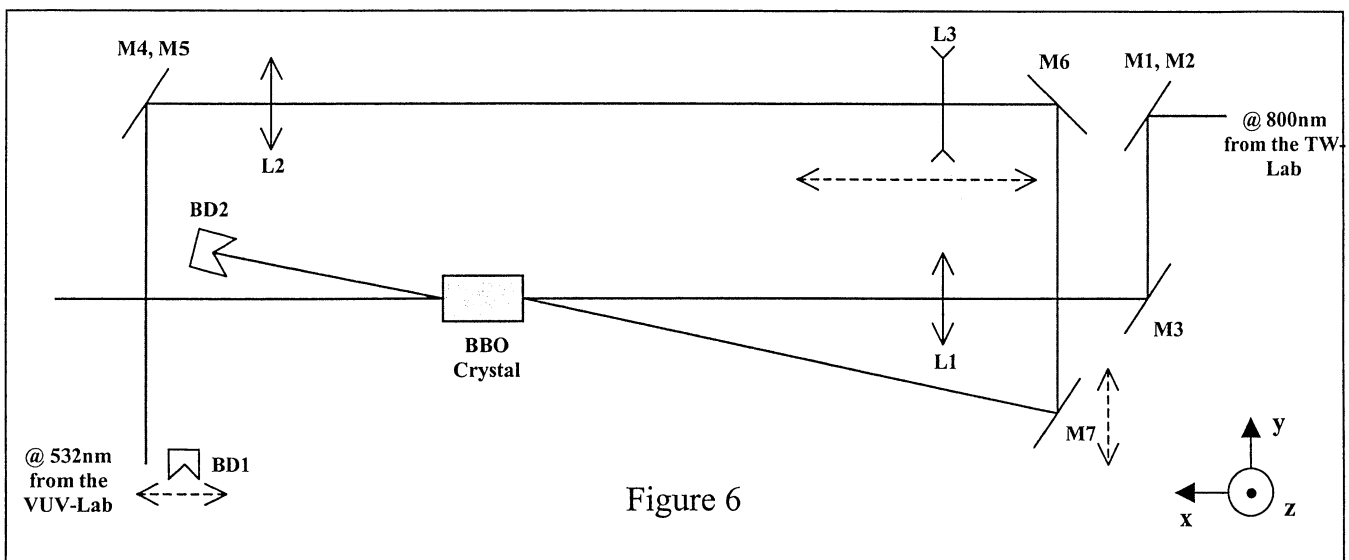
Remark

#### - Signal beam:



The signal laser beam comes from the TeraWatt-Lab (upper right corner of Figure 5). The polarization of this beam is horizontal, but it must be vertical into the crystal. The mirrors M1 and M2 are used to change the polarization. The incoming signal beam that propagates along the x-axis is reflected on M1 and follows afterwards the z-axis, while mirror M2 reflect this z-axis propagating beam onto the y-axis. After this combination of mirrors our beam is vertically polarized and ready to be focused into the crystal. The position of the following mirror M3 has been determined so that the signal beam has the right injection angle into the crystal i.e. 0,018 degree. L1 finally focuses the beam into the center of the crystal with a diameter of 0,25 mm.

- Pump beam:



The pump beam comes from the VUV-Lab (bottom left of Figure 6) and has a vertical polarization while we need a horizontal one in the crystal. The same kind of mirror association than M1 and M2 is used to turn the polarization. Thus M4 reflects the incoming pump beam that initially follows the y-axis so it lays afterwards parallel to the z-axis, M5 reflects this z-axis orientation beam to the  $-x$  direction. The pump beam is thereafter horizontally polarized and can be positioned such as it goes into the crystal with the right angle (M6 and M7). Between the M4, M5 combination mirrors and M6 lays down a telescope made of one positive lens L2 and one negative lens L3. The aim of this lens system is to form a long effective focal length optics to focus the pump beam into the crystal.

It is important to notice that some components (L3 and M7) can be moved - (x-translation and y-translation respectively for L3 and M7 see dashed arrows in Figure 6). The translation of L3 allows us to optimize the focusing position of the pump beam while the y-axis translation of M7 allows us to optimize the overlapping of the two beams into the BBO crystal without changing the angle of non-collinearity.



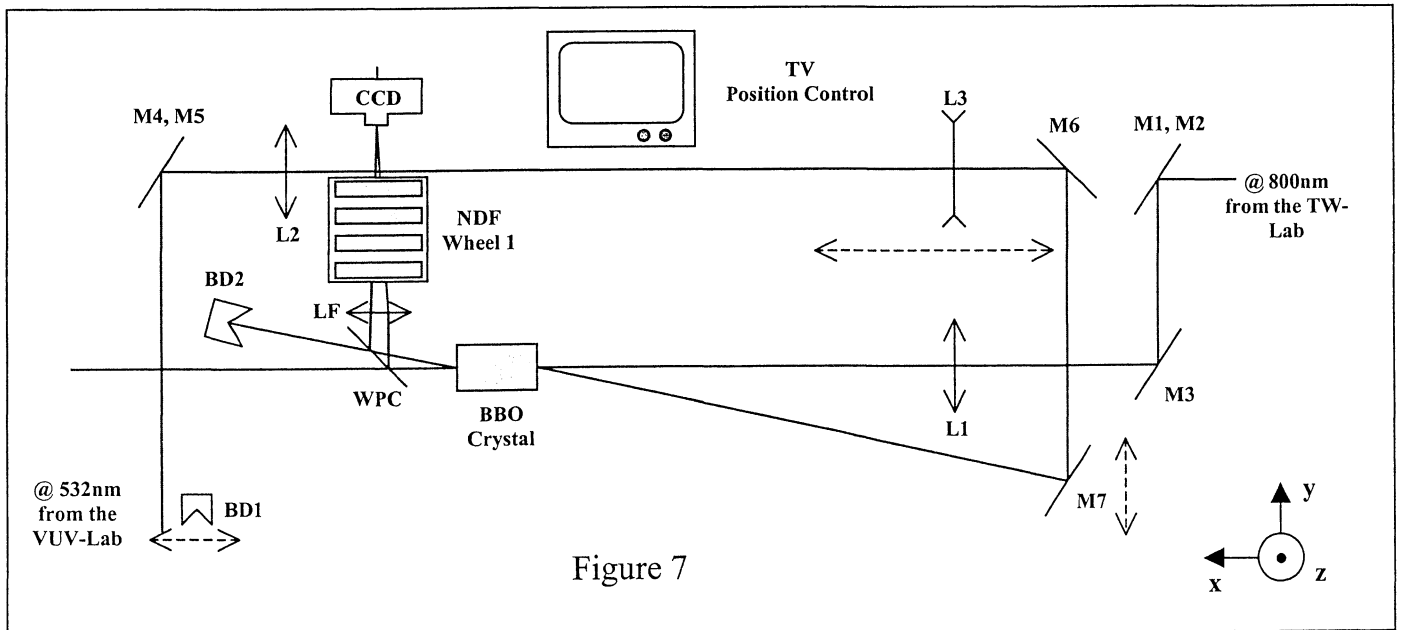
The components BD1 and BD2 are two beam dumpers and are used to stop the propagation of the pump beam. BD1 has been implemented for safety reasons. It can be placed in the optical pathway of the pump beam to prevent it to enter in the optical system. BD2 just stops the propagation of the pump beam after the non-linear crystal.

Remark

In addition an iris was placed in the VUV-Lab to vary the diameter of the pump beam inside the crystal. Without this iris the diameter of the pump beam was about 0,6 mm which is too small in comparison to the 0,2 mm diameter of the signal beam for a good overlapping of the two beams. The incoming beam in the VUV-Lab was apertured down from 1 cm to 5 mm diameter thus increasing the diameter of the focused pump beam in the crystal to a value of 0,9 mm. This value of 5 mm (i.e. 0,9 mm in the crystal) was the best compromise between the efficiency of overlapping and the intensity that the non-linear crystal is exposed to.

- Monitoring system:

After having aligned the two beams, we had to check their sizes and positions in the crystal. The crystal was replaced by a pinhole of 0,5 or 1 mm diameter and the beams were positioned so they passed through the hole. A wedge plate WPC was placed behind the crystal to split the two beams and the pinhole was imaged with a lens LF on a CCD camera after a Neutral Density Filters Wheel (NDF Wheel) as shown in Figure 7:



- Degrees of Freedom of the Crystal:

We saw in the previous paragraphs that some of the optical components of the experiment (L3, M7 BD1 etc ...) could be moved. It was important that the crystal could be translated and rotated in several ways. For this purpose, a special mount was design to allow five operations:

1 Rotation around z

This is one of the most important operation since it allowed us to adjust the phase-matching angle of the beams into the crystal.

2,3 Rotations around x and y

The reflection of the beams on the front surface of the crystal could be adjusted.

4,5 Translations along y and z axes

The crystal used was damaged in three different places so these translations were very useful to select a clean area of the crystal. Furthermore the translation along the y-axis was also used to “switch” easily between the crystal and the pinhole without removing it.

## Measurement of the Spectral Gain

### Introduction to the Measurements



With the present setup we could look for a gain by adjusting the position of several components such as L3, M6, M7 or the crystal .This first experiment used a seeded pump laser with 15mJ energy into the crystal.

*The transmission of the pump laser optical pathway is about 80% and there is a reflection on the front surface of the crystal of a few percents. So the output energy of the pump laser in the VUV-Lab is 75% higher than in the crystal. Thus for 15 mJ in the crystal, we need an output energy of 20 mJ that is far below the maximum output energy of this Nd:YAG laser of 700 mJ/pulse.*

Remark

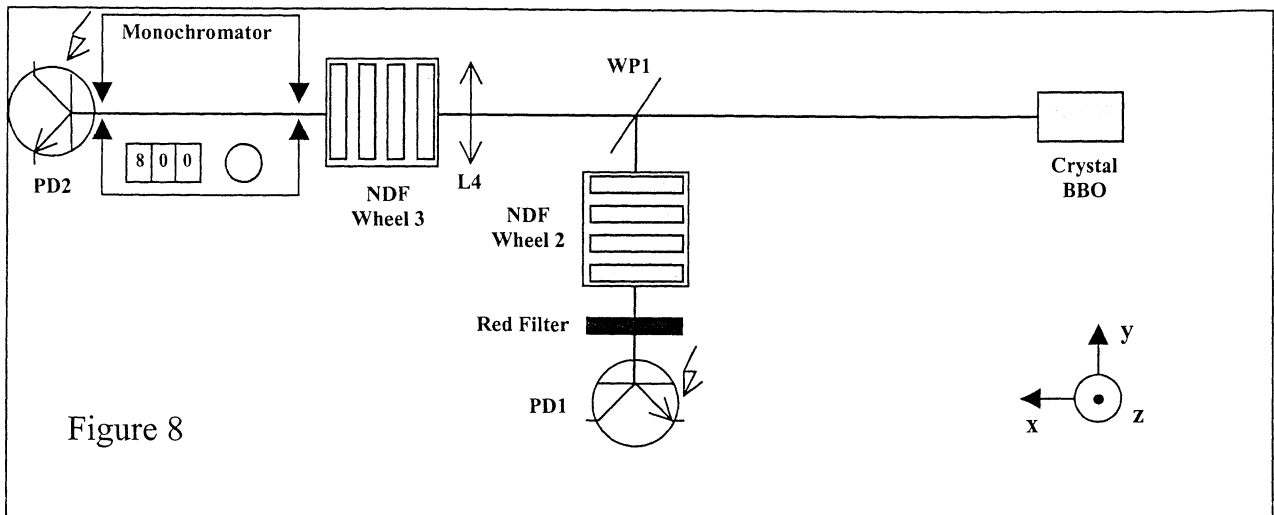


Figure 8

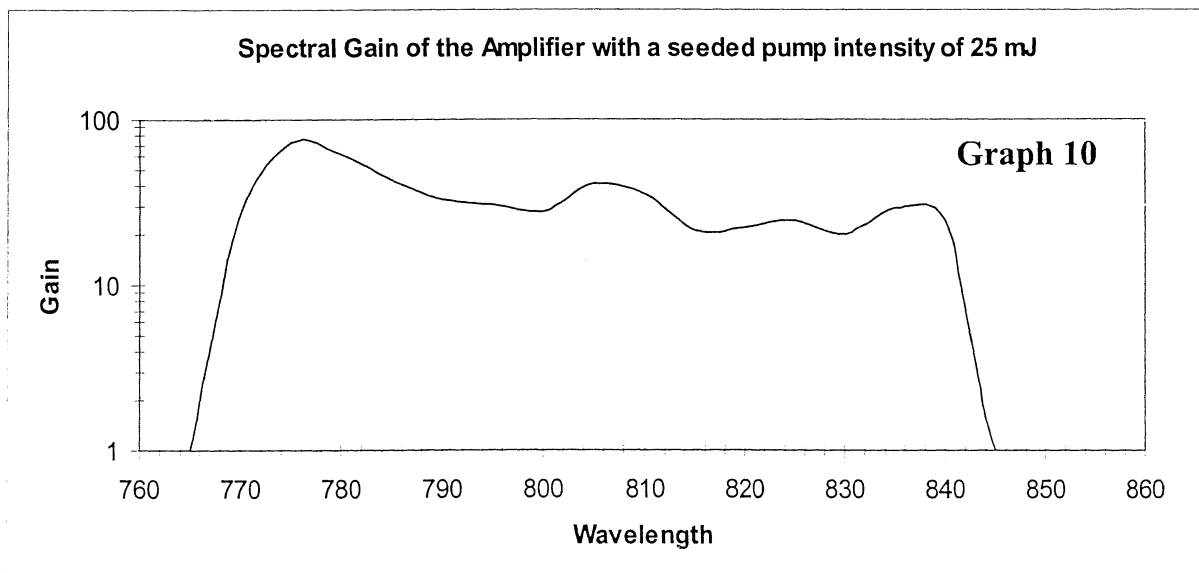
To be able to measure the gain I set up a photodiode (PD1) was placed behind by a wedge plate (WP1). A Neutral Density Filter Wheel (NDF Wheel2) and a red filter that cuts totally the green light of the pump laser that were used to avoid saturation

The main part of the signal beam was transmitted by WP1 and focused by a 100 mm focal length lens (L4) into a monochromator. This optical component separates the different wavelengths and allows us to study the spectral gain with the use of a second photodiode (PD2). A Neutral Density Filters Wheel (NDF Wheel 3) before the monochromator was also used to avoid the saturation of the photodiode.

Amplification with the Seeded pump laser

The positions of the two beams and of the crystal were adjusted in order to observe some gain with PD1. Amplification was obtained with an angle of non-collinearity very close to the theoretical one.

However, it was not possible to obtain a higher gain than 500 using up to 25mJ pump energy in the crystal. The spectral gain measured (see below) was broad over 70 nm.



The possible reasons for this low gain are:

- the signal and pump beams were not perfectly overlapping into the crystal
- the theoretical model “missed” some effects resulting in lower effective gain.

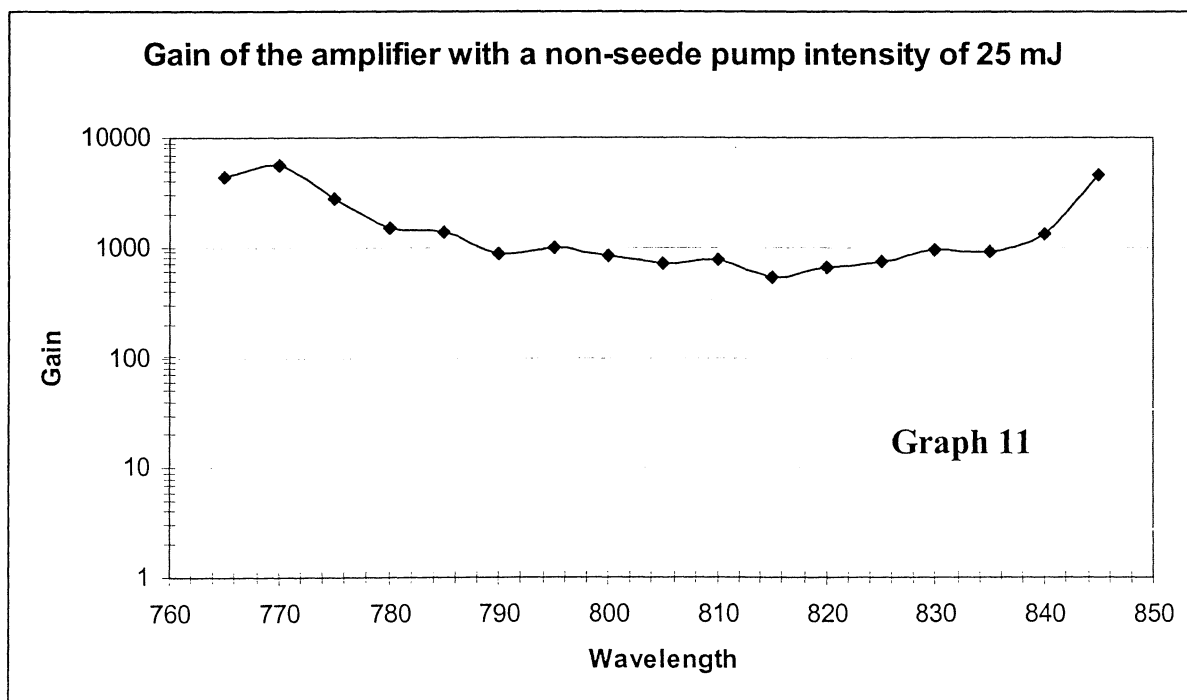
To compensate for them, a further considerable increase of pump energy could have been necessary, which, however, might have damaged the crystal. Please note that the damage of crystal is fluence-dependent while the amplification is intensity dependent. That’s why it is more preferable to use shorter pump pulses in actual OPCPA system whose duration is close to the duration of the signal pulse.

### Amplification with the Unseeded pump laser

Using a unseeded pump laser, the temporal shape of the pulse becomes spiky as seen previously on Graph 7. These spikes represent considerably higher pump intensity for the same temporally integrated pump energy than for the seeded case. The pump beam was moving a little bite more than before. With this new configuration, I achieve a much higher amplification.

An amplification higher than 4000 with an energy of 32 mJ inside the crystal was achieved. The trade off is that the amplification system loses in stability.

The measurement of the gain as a function of wavelength is presented below:





Now to calculate the gain we consider that:

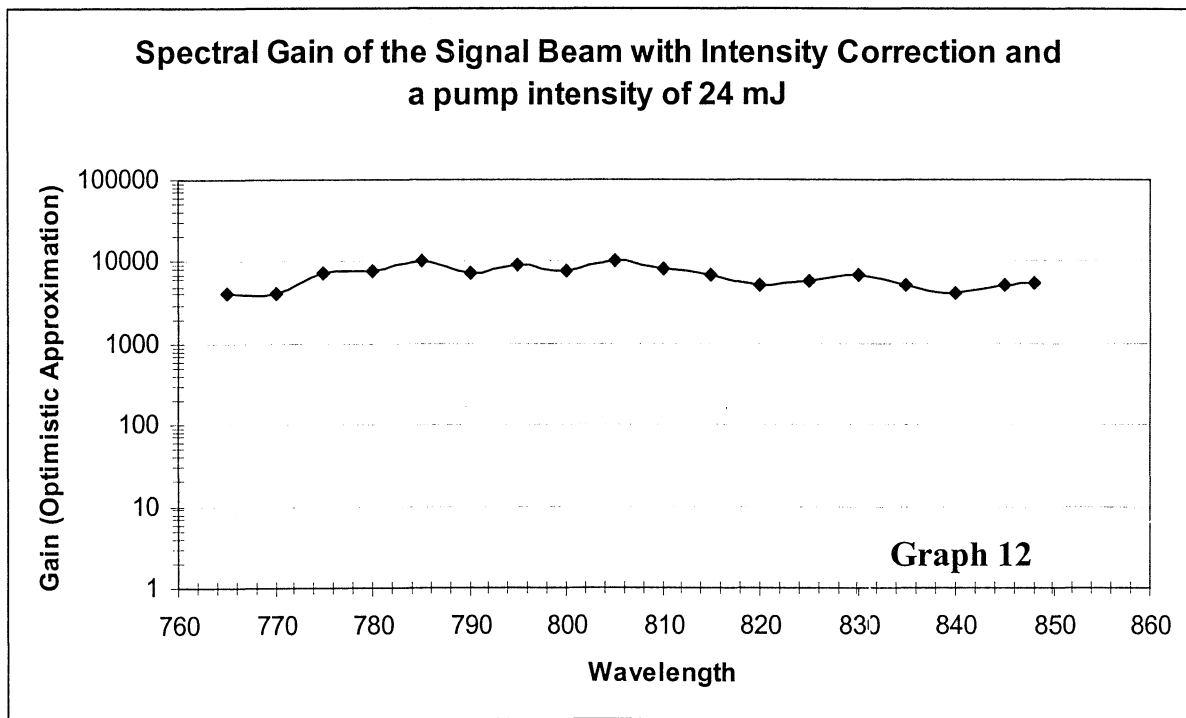
$$\frac{I_{\text{sampli}}}{I_s} \propto \exp[I_p]$$

Where  $I_{\text{sampli}}$  is the intensity of the amplified beam  
 $I_s$  the intensity of the incoming signal beam  
 $I_p$  the intensity of the pump beam

We can now introduce a normalized value of the pump intensity  $I_p^n$  so we could calculate the gain according to:

$$\text{Gain} = \frac{I_{\text{sampli}}}{I_s} \cdot \exp[I_p^n]$$

The result of this second series of measures is represented on the following graph:



We can immediately see the improvement between this new graph and graph 11. The previous one was hollowed out in its middle while this one is almost flat. This is a very good result since a flat spectral gain over this entire spectral window is a requirement to get a short pulse.

## Compression of the pulse

### Introduction about the compression

The compression of the pulse amplified by an OPCPA is as important as the amplification itself. In fact, this amplifier is not interesting if we can not recompress the pulse to its transform limit.

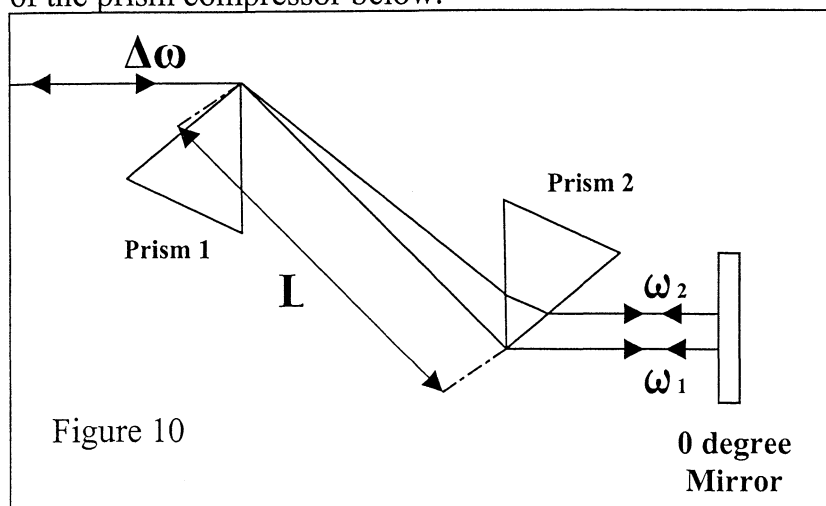
The signal pulse has been stretched by going into a dispersive medium with a large Group-Velocity dispersion. Moreover, it has been deviated and reflected on optical supports such as mirrors or wedge plates etc... that exhibit **positive** Group-Delay Dispersion GDD and higher order dispersion such as Third Order Dispersion TOD (also known as Cubic Dispersion CD). The phase of the pulse can be written as:

$$\phi(\omega) = \phi(\omega_0) + GD \cdot \Delta\omega + \frac{1}{2} \cdot GDD \cdot \Delta\omega^2 + \frac{1}{6} \cdot TOD \cdot \Delta\omega^3 \quad \Delta\omega = \omega - \omega_0$$

A **negative** GDD and to a less extend a negative TOD are require to recompress the stretched-in-time and chirped pulse. We decided to use a sequence of antiparallel prisms at Brewster angle compressor in order to recompress our signal pulse.

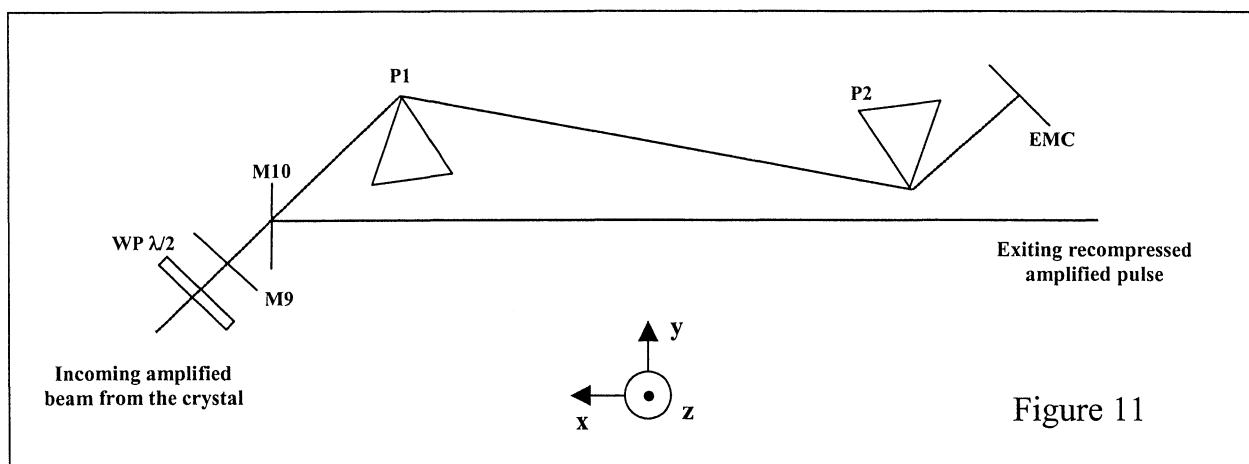
### Prism Compressor

A prism compressor is a good solution to provide a negative and controllable GDD as well as to reduce the TOD. The prisms are used at minimum deviation (i.e. with incidence angle equal to the exit angle) and are cut in such a way that the input rays enter and leave the prisms at Brewster's angle. Moreover the exit surface of the first prism is parallel to the entrance surface of the second one. We can see a representation of the prism compressor below:



In Figure 10,  $\Delta\omega$  represents the incoming stretched-in-time broadband pulse that is deviated by the first prism. Every frequency is spread spatially ( $\omega_1 < \omega_2$ ) and deviated by the second prism. The mirror reflects the spread beam that travels the same way back and finally finds its initial size back. This sequence introduces a negative and controllable GDD and TOD, by changing the distance  $L$  between both prisms, this allowing the recompression of the beam.

The compressor was built in a double passes configuration. It means that the beam make two complete passes into the prism compressor. The setup is shown below:



The incoming amplified beam is coming from the crystal (bottom left of Figure 11) and is vertically polarized. For such a polarization the reflections on each front surface of the prism compressor are maximal. We changed the polarization with a  $\lambda/2$  0-order wave-plate. Then the beam enters the compressor and makes a complete trip into it. It goes through P1, P2, reflect on the end mirror of the compressor EMC and goes again through P2 and P1. After this first trip, the beam is reflected by M9 so it enters again in the compressor in order to complete another trip. Finally after this second pass through the compressor, the recompressed beam hits the mirror M10 and reflect it in the direction of the rest of the setup.

The next step of the experiment is to measure the width of the pulse in order to determine if the distance between the two prisms is optimal and in a second time if the pulse can be recompressed to its transform limit.

### Autocorrelation of the Pulse

To carry out the autocorrelation of the compressed pulse we had at our disposal two autocorrelators: multi-shot and single-shot. The multi-shot autocorrelator was used to find roughly the optimum distance between the two prisms (i.e. the best recompression).



Autocorrelator Multi-shot

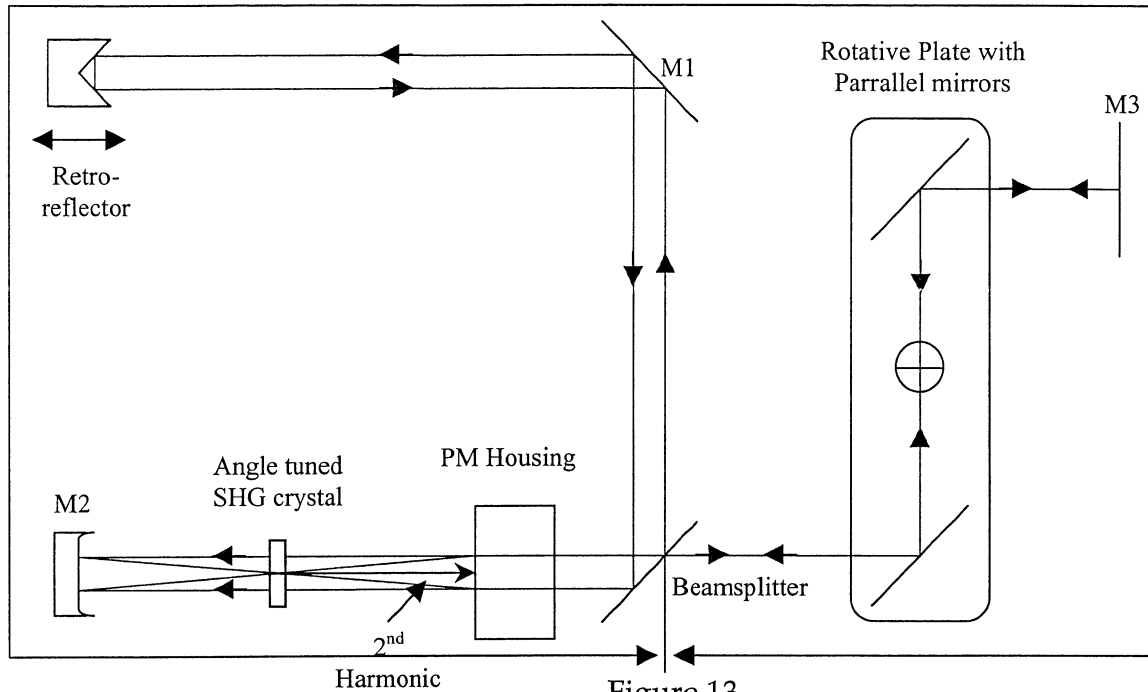


Figure 13

The incoming beam enters the autocorrelator through the adjustable aperture at the bottom of Figure 13. After the beam splitter, part of the beam continues its way up to the mirror M1 to make a round trip M1, retro-reflector, M1 again and comes back to the beam splitter that will reflect part of this beam onto the focusing mirror M2. At the same time, the second part of the incoming beam make a round trip on the right arm of the autocorrelator, goes to the parallel mirrors mounted on a rotating plate, then hits the mirror M3 before going back through the beam splitter to the focusing mirror M2. Both beams are focused into the angle tuned SHG crystal that delivers a second harmonic signal. The width information contained by this 2<sup>nd</sup> harmonic beam is finally collected by the photo-multiplier and visualized on an oscilloscope.

After a rough optimization of the setup we obtained a signal with a pulse width of 55 fs and tried to get a better result using the single-shot autocorrelator and trying to compensate more the GDD and the residual TOD.

Autocorrelator Single-shot

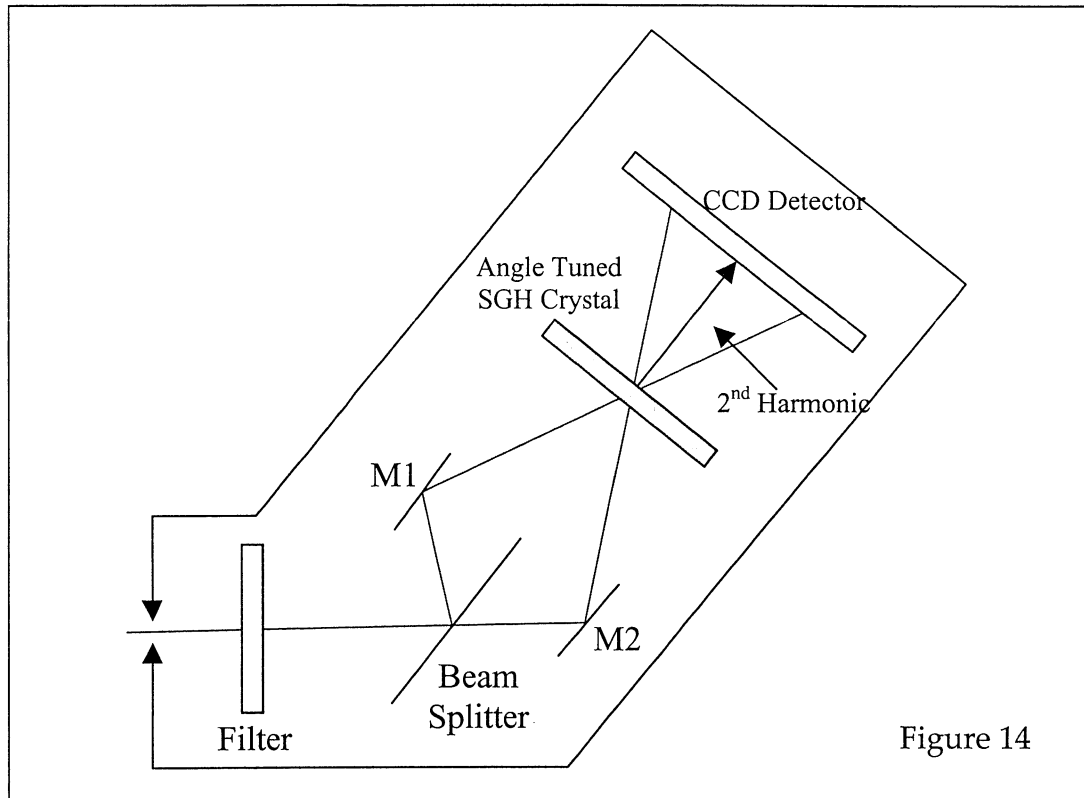
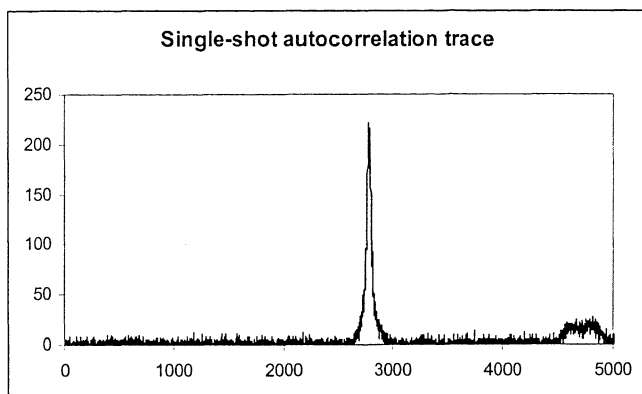


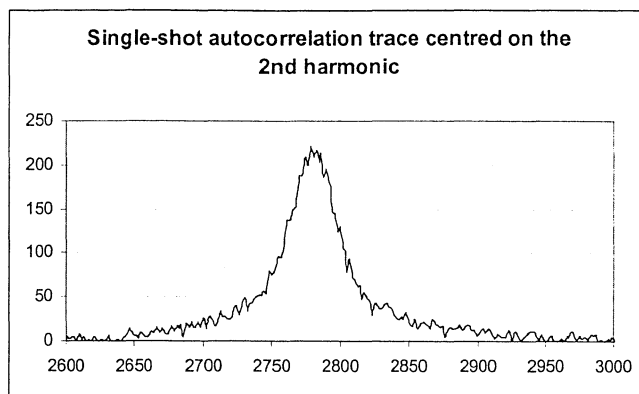
Figure 14

The principle of this autocorrelator is different in the sense that there is a CCD detector and not a photo-multiplier to detect the presence of the second harmonic generated by an angle-tuned SHG crystal. We don't need any rotating element. After the entrance aperture of the autocorrelator stand a filter and a thin beam splitter that divides the incoming beam in two parts. These two replicas go respectively on mirror M1 and M2, are reflected and interact in the crystal where the second harmonic is generated. The temporal resolution of the device is determined by the angle between the two beams.

After optimizing the alignment of the autocorrelator and after tuning the angle of the beam splitter and of the crystal, we obtained a second harmonic signal from the coupling of the two incident beams. So the distance between the prisms was optimized in order to achieve a width of 40 fs for the recompressed pulse. This width is not the optimal length of the transform limit pulse. There is a pedestal on the shape of the single-shot autocorrelation trace which may be a sign of some non-compensated TOD (see the graphs below).



Graph 11



Graph 12

## Discussion and Conclusion

### Discussion about the experiment

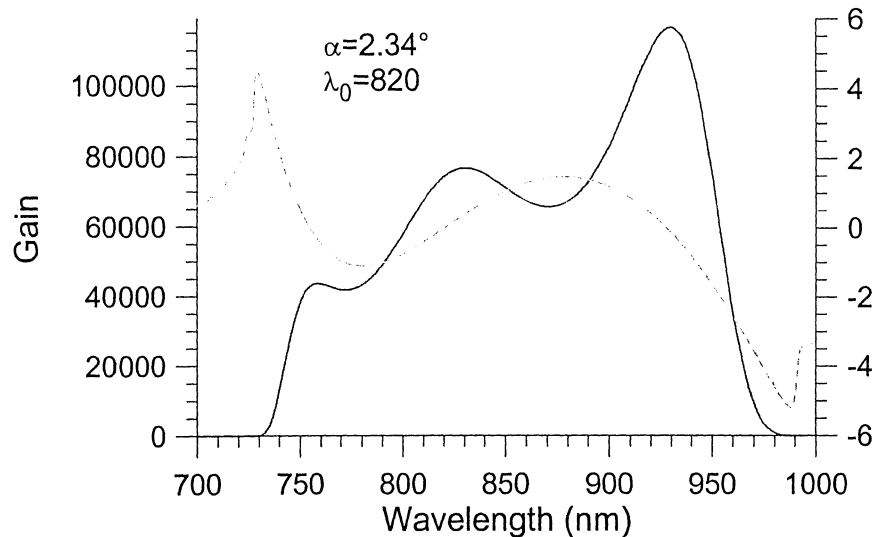
The calculations and experiment I performed during those six months and described in this report has allowed me to obtain some interesting results. With the seeded pump Nd:YAG laser, I achieved a stable but weak 70 nm broadband amplification. However, by switching off the seeder of the pump laser, it was possible to reach a gain of several thousand on a very broad bandwidth which unfortunately was rather unstable mainly due to the randomly distributed in time intensity of the pump laser.

A sequence of Brewster's prisms was set up to compensate for the positive delay dispersion and chirp introduced in the signal beam. The compressor and the measurement tools behind it (i.e. multi and single-shot autocorrelators) were aligned. A recompress signal pulse of 40 fs without amplification was obtained. This value of 40 fs seems to be quite good if we consider that the third-order dispersion had not been efficiently corrected. To go further other geometries of prism compressor would have been studied, with other glass materials<sup>(10)</sup> or fine tuning processes<sup>(11)</sup>. It could also have been possible to change the dielectric 0-degree 800 nm end mirror of the compressor by a chirped mirror exhibiting a better compensation for the third-order dispersion.

However, it has not been possible to measure the pulse width of the amplified beam. The instability of the amplification made this measurement difficult to perform with the present experiment setup. The amplification reaches a value higher close to 10000 (i.e. a signal intensity of about 40  $\mu\text{J}$ ) approximately every ten or twenty seconds with several amplifications peaks higher than 5000 in between. During the same time the eighty millions shots of the non-amplified signal makes the measurements of the amplified beam's width too difficult.

It is of course possible to improve the experiment. A Pockels cell correctly triggered could be used to clean the amplified signal from the 80 MHz not amplified signal. It would be nice to turn on the seeder again and to manage to amplify the signal beam with this seeded mode of radiation of the pump laser possibly using a higher energy. With the experience I accumulate working on the amplification with the not-seeded pump beam, I feel now able to reach a good amplification with the seeded pump laser. But unfortunately the time I have at my disposal is not big enough to lead a serious experiment.

I believe that the amplified beam obtained with the unseeded pump laser could be recompressed to its transform limit width. We saw that the amplification was very flat. It means that we did not reach the wings of the amplification where the phase modulation is very important and makes the amplified signal impossible to recompress perfectly. On the graph beneath we can observe the evolution of the phase and of the amplification for another OPCPA experiment performed by Karoly Osvay:



We can finally see the whole experiment scheme given at the end of the report; see Experimental Setup.

### Conclusion about this training period

As a conclusion I would like to give you my personal point of view about everything that happened here in Lund. First, the working experience I have accumulated seems to me tremendous. By meeting very good scientists during the conferences and the Friday meetings organized at the LLC and in the Division of Atomic Physics, I learned a lot and developed my knowledge about very hot topics. But above all, I met during every working day very nice and competent scientists that are also very nice persons. They transmitted me much more than simple knowledge ... They gave me their own experience, their own skills, and their love of Science. I am sure that I will never forget those wonderful persons.

Now as a person, I had the chance to meet a lot of Swedish people and international students. It has been a pleasure to share everything we had and discover what was common between all of us. I really appreciate Sweden and Skåne, the charm of the countryside, the beautiful landscapes, the long white-sand beach of Sandhammar, the Swedish language, and all the rest. This training period has been for me a complete success. Moreover I manage to increase my level in English that was originally the main aim of this trip abroad.

More than a training period, it has been a living period.

## List and description of the optical components

Lens	Material / Quality / Manufacturer	Focal Length	Geometry
L1	pcv0309	700	Planar-Convex
L2	BK7, ar 532 nm	1000	Planar-Convex
L3	ar 532 nm	-250	Planar-Concave
L4	----	100	----
L5	ar 532 nm	200	Planar-Convex
L6	pcx0302	-50	Planar-Concave
LF		480	----

Mirror	Specification
M1	800 nm, 45°, dielectric
M2	Gold
M3	Gold
M4	532 nm, 45°, dielectric
M5	532 nm, 45°, dielectric
M6	532 nm, 45°, dielectric
M7	532 nm, 45°, dielectric
M8	800 nm, 45°, S polarisation
M9	Gold
M10	Gold
MRC	Gold
EMC	800 nm, 0°, dielectric

Wedge Plate	Quality	Thickness	Diameter
WP1	$\lambda/10$	----	50.8
WP2	3 deg	0.5"	38.1
WP3	3 deg	0.375'	25.4

Photodiode	Response Time
PD1	1 ns
PD2	2.5 ns
PD3	1 ns

## References

1. A. Dubietis, G. Jonusaukas, and Piskarskas, Optics Communications **88**, 437 (1992).
2. I.N. Ross, P. Matousek, M. Towrie, A.J. Langley, and J.L. Collier, Optics Communications **144**, 125 (1997).
3. H. Yoshida, E.Ishii, R. Kodama, H. Fujita, Y. Kitagawa, Y. Izawa, and T. Yamanaka, Optics Letters **28**, 257 (2003)
4. I.N. Ross, J.L Collier, P. Matousek, C.N Danson, D. Neely, R.M Allot, D.A. Pepler, C.Hernandez-Gomez, and Karoly Osvay, Applied Optics **39**, 2422 (2000)
5. I. Jovanovic, B.J. Comaskey, and D.M. Pennigton, Applied Physics **90**, 4328 (2001)
6. E. Ibragimov, A. Stuthers, and D.J. Kaup, Optical Society of America, **18**, 1872 (2001)
7. X. Yang, Z. Xu, Z. Zhang, Y. Leng, J. Peng, J. Wang, S. Jin, W. Zhang, and R. Li, Applied Physics **73**, 219-222 (2001)
8. S.K. Zhang, M. Fujita, M. Yamnaka, M. Nakatsuka, Y. Izawa, and C. Yamanaka, Optics Communications **184**, 451-455 (2000)
9. J.A. Armstrong, N. Bloembergen, J. Docuing, and P.S Pershan, Physics Review **127**, 1918 (1962)
10. R.E. Sherriff, Optical Society of America **15**, 1224 (1998)
11. K. Osvay, P. Dombi, A.P. Kovács, Z. Bor, Applieds Physics B **75**, 649-654 (2002)

## **Annexe I - Calculations**

This first annexe gives an overview of the calculations. This work had been made during the two first months with the help of MathCad software.

The units used in this program are usually neither SI nor csg but just common units for the calculation.



## Study of parameters for a NOPCPA

$$\theta := 26.1 \text{ deg}$$

$$\mu\text{m} := 0.001 \text{ mm} \quad \text{GW} := 10^9 \text{ watt}$$

### Energy conservation:

$$\lambda_p := 0.532 \quad \lambda_s := 0.800$$

$$\lambda_i := (\lambda_p^{-1} - \lambda_s^{-1})^{-1}$$

$$\lambda_i = 1.588$$

### Refractive Index: Sellmeier Equation:

$$n_{po} := \sqrt{2.7359 + \frac{0.01878}{\lambda_p^2 - 0.01822} - 0.01354 \cdot \lambda_p^2}$$

$$n_{po} = 1.674$$

$$n_{pe} := \sqrt{2.3753 + \frac{0.01224}{\lambda_p^2 - 0.01667} - 0.01516 \cdot \lambda_p^2}$$

$$n_{pe} = 1.555$$

$$n_{so} := \sqrt{2.7359 + \frac{0.01878}{\lambda_s^2 - 0.01822} - 0.01354 \cdot \lambda_s^2}$$

$$n_{so} = 1.661$$

$$n_{io} := \sqrt{2.7359 + \frac{0.01878}{\lambda_i^2 - 0.01822} - 0.01354 \cdot \lambda_i^2}$$

$$n_{io} = 1.646$$

### Determination of the Phase-Matching Angle $\theta$ :

$$\theta\theta := 21 \text{ deg} \quad n_p(\theta) := \sqrt{\left( \frac{\cos(\theta)^2}{n_{po}^2} + \frac{\sin(\theta)^2}{n_{pe}^2} \right)^{-1}}$$

$$\alpha_1 := 2.34 \text{ deg}$$

Given

$$np(\theta) = \sqrt{\lambda_p^2 \left[ \frac{n_{io}^2}{\lambda_i^2} + \frac{n_{so}^2}{\lambda_s^2} + \frac{2 \cdot n_{io} \cdot n_{so}}{\lambda_i \cdot \lambda_s} \cdot \left[ \sqrt{1 - \left( \frac{n_{so} \cdot \lambda_i}{n_{io} \cdot \lambda_s} \cdot \sin(\alpha_1) \right)^2} \cdot \cos(\alpha_1) - \frac{n_{so} \cdot \lambda_i}{n_{io} \cdot \lambda_s} \cdot \sin(\alpha_1) \right]^2 \right]}$$

$$\theta_c := \text{Find}(\theta)$$

$$\theta_c = 23.771 \text{ deg} \quad np(\theta_c) = 1.653$$

### Angle Outside the Crystal :

$$\alpha_{out} := \text{asin}(n_{pe} \cdot \sin(\alpha_1)) \quad \alpha_{out} = 3.639 \text{ deg}$$

### Angle Outside the Crystal with cut angle of the Crystal :

$$\alpha_{out2} := \text{asin}(n_{pe} \cdot \sin(\theta - \theta_c)) \quad \alpha_{out2} = 3.623 \text{ deg}$$

$$is := \theta - \theta_c - \alpha_1 \quad is = -0.011 \text{ deg}$$

$$is_{out} := \text{asin}(n_{so} \cdot \sin(is)) \quad is_{out} = -0.018 \text{ deg}$$

### Phase-Matching as a function of the Wavelength:

#### Functions and Variables:

$$\lambda_{li}(\lambda\lambda) := (\lambda_p^{-1} - \lambda\lambda^{-1})^{-1}$$

$$n_s(\lambda\lambda) := \sqrt{2.7359 + \left( \frac{0.01878}{\lambda\lambda^2 - 0.01822} \right) - 0.01354 \cdot \lambda\lambda^2}$$

$$ni(\lambda\lambda) := \sqrt{2.7359 + \left[ \frac{0.01878}{\left[ \left( \lambda_p^{-1} - \lambda\lambda^{-1} \right)^{-1} \right]^2} - 0.01822 \right]} - 0.01354 \cdot \left[ \left( \lambda_p^{-1} - \lambda\lambda^{-1} \right)^{-1} \right]^2$$

$$\alpha\alpha2(\lambda\lambda) := \text{asin} \left( \frac{ns(\lambda\lambda)}{\lambda\lambda} \cdot \frac{\lambda\lambda i(\lambda\lambda)}{ni(\lambda\lambda)} \cdot \sin(\alpha1) \right)$$

$$\Delta\Delta k(\lambda\lambda) := \frac{2 \pi \cdot np(\theta c)}{\lambda p} - \frac{2 \pi \cdot ns(\lambda\lambda)}{\lambda\lambda} \cdot \cos(\alpha1) - \frac{2 \pi \cdot ni(\lambda\lambda)}{\lambda\lambda i(\lambda\lambda)} \cdot \cos(\alpha\alpha2(\lambda\lambda))$$

**Defining of Vectors:**

```

lambda_s(lambda_min, lambda_max, lambda_step) :=
  count ← 0
  for lambda ∈ lambda_min, lambda_min + lambda_step .. lambda_max
    v_count ← lambda
    count ← count + 1
  v

```

+

```

lambda_i(lambda_min, lambda_max, lambda_step) :=
  count ← 0
  for lambda ∈ lambda_min, lambda_min + lambda_step .. lambda_max
    v_count ← lambda_i(lambda)
    count ← count + 1
  v

```

```
nso( $\lambda$ min,  $\lambda$ max,  $\lambda$ sstep) := | count ← 0
                             | for  $\lambda \in \lambda$ min,  $\lambda$ min +  $\lambda$ sstep..  $\lambda$ max
                             | |  $v_{count} \leftarrow ns(\lambda)$ 
                             | | count ← count + 1
                             | v
```

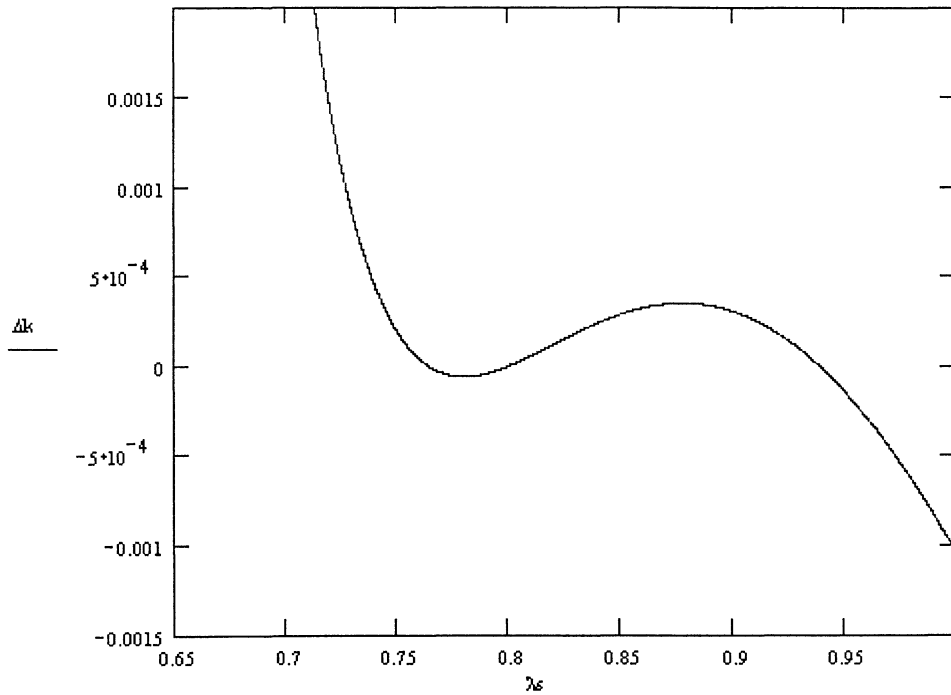
```
nio( $\lambda$ min,  $\lambda$ max,  $\lambda$ sstep) := | count ← 0
                             | for  $\lambda \in \lambda$ min,  $\lambda$ min +  $\lambda$ sstep..  $\lambda$ max
                             | |  $v_{count} \leftarrow ni(\lambda)$ 
                             | | count ← count + 1
                             | v
```

```
o2( $\lambda$ min,  $\lambda$ max,  $\lambda$ sstep) := | count ← 0
                              | for  $\lambda \in \lambda$ min,  $\lambda$ min +  $\lambda$ sstep..  $\lambda$ max
                              | |  $v_{count} \leftarrow \alpha 2(\lambda)$ 
                              | | count ← count + 1
                              | v
```

```
 $\Delta k$ ( $\lambda$ min,  $\lambda$ max,  $\lambda$ sstep) := | count ← 0
                                   | for  $\lambda \in \lambda$ min,  $\lambda$ min +  $\lambda$ sstep..  $\lambda$ max
                                   | |  $v_{count} \leftarrow \Delta \Delta k(\lambda)$ 
                                   | | count ← count + 1
                                   | v
```

$$\Delta k := \Delta k(0.600, 1.000, 0.0001)$$

$$\lambda_s := \lambda_s(0.600, 1.000, 0.0001)$$



### Study and Optimisation of the Gain:

#### Defining Variables and functions :

$$d22 := 2.3 \cdot 10^{-6}$$

$$d31 := 0.16 \cdot 10^{-6}$$

$$\phi := \frac{\pi}{2}$$

$$deff := d31 \cdot \sin(\theta c) - d22 \cdot \cos(\theta c) \cdot \sin(3 \phi)$$

$$deff = 2.169 \cdot 10^{-6}$$

$$I_p := 10$$

$$g0 := 8.85 \cdot 10^{-6}$$

$$L := 14000$$

$$c := 299.79245800$$

$$gg(\lambda\lambda) := 4 \cdot \pi \cdot \text{deff} \cdot \frac{I_p}{\sqrt{2 \cdot \varepsilon_0 \cdot \text{np}(\theta c) \cdot \text{ns}(\lambda\lambda) \cdot \text{ni}(\lambda\lambda) \cdot c \cdot \lambda\lambda \cdot \lambda\lambda i(\lambda\lambda)}}$$

$$\text{GGain}(\lambda\lambda) := 1 + gg(\lambda\lambda)^2 \cdot \frac{\sinh \left[ L \cdot \sqrt{gg(\lambda\lambda)^2 - \left( \frac{\Delta\Delta k(\lambda\lambda)}{2} \right)^2} \right]^2}{gg(\lambda\lambda)^2 - \left( \frac{\Delta\Delta k(\lambda\lambda)}{2} \right)^2}$$

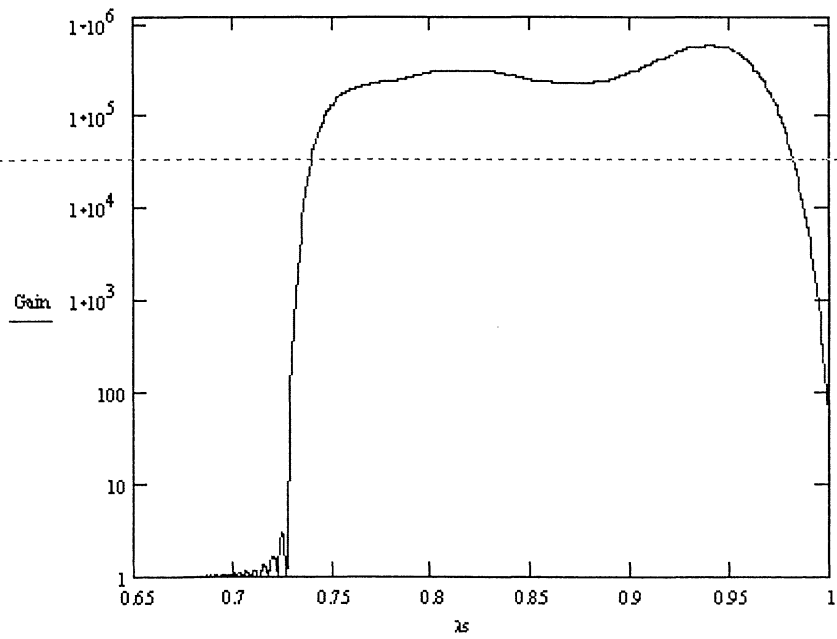
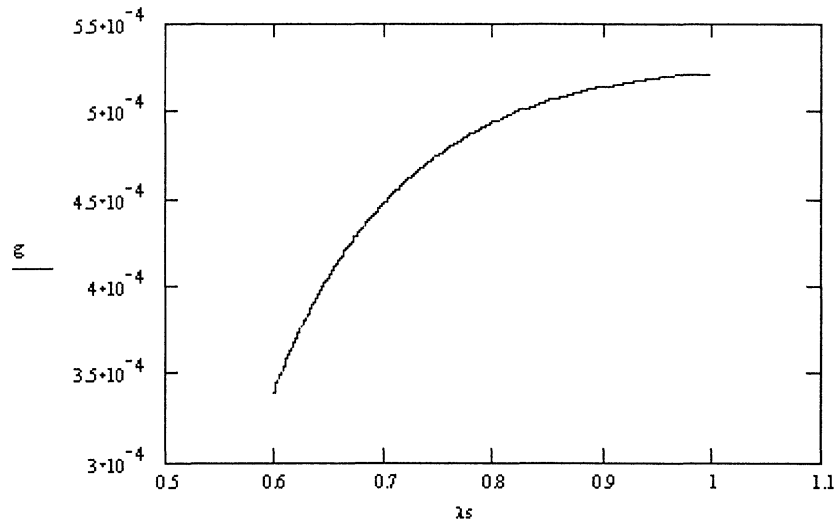
### Defining Vectors :

$$g(\lambda\text{min}, \lambda\text{max}, \lambda\text{step}) := \begin{array}{l} \text{count} \leftarrow 0 \\ \text{for } \lambda\lambda \in \lambda\text{min}, \lambda\text{min} + \lambda\text{step} .. \lambda\text{max} \\ \quad \left| \begin{array}{l} v_{\text{count}} \leftarrow gg(\lambda\lambda) \\ \text{count} \leftarrow \text{count} + 1 \end{array} \right. \\ v \end{array}$$

$$\text{Gain}(\lambda\text{min}, \lambda\text{max}, \lambda\text{step}) := \begin{array}{l} \text{count} \leftarrow 0 \\ \text{for } \lambda\lambda \in \lambda\text{min}, \lambda\text{min} + \lambda\text{step} .. \lambda\text{max} \\ \quad \left| \begin{array}{l} v_{\text{count}} \leftarrow \text{GGain}(\lambda\lambda) \\ \text{count} \leftarrow \text{count} + 1 \end{array} \right. \\ v \end{array}$$

Gain := Gain(0.600, 1.000, 0.0001)

g := g(0.600, 1.000, 0.0001)



$$\max(\text{Gain}) = 5.025 \cdot 10^5$$

$$\text{Gain}_{2000} = 2.54 \cdot 10^5$$

**Biréfringence Walk-Off angle  $\rho$ :**

$$\rho := \text{atan} \left[ \left( \frac{n_{po}}{n_{pe}} \right)^2 \cdot \tan(\theta_c) \right] - \theta_c$$

$$\rho = 3.287 \text{ deg}$$

$$\rho_1 := \text{atan} \left[ \frac{n_p(\theta_c)^2}{2} \cdot \left( \frac{1}{n_{pe}^2} - \frac{1}{n_{po}^2} \right) \cdot \sin(2 \cdot \theta_c) \right]$$

$$\rho_1 = 3.287 \text{ deg}$$

**Real angle between the pump and signal beam:**

$$\alpha := \rho - \alpha_1$$

$$\alpha = 0.947 \text{ deg}$$

+

**Deviation of the signal beam compared with the pump beam:**

-----  
**Defining angles and lengths :**

$$s := \theta - \theta_c + \alpha_1 \quad s = 4.669 \text{ deg}$$

$$l_1 := \frac{L}{2} \cdot \tan(s) \quad l_1 = 571.743$$

$$sp := \theta - \theta_c + \rho \quad sp = 5.616 \text{ deg}$$

$$l_2 := \frac{L}{2} \cdot \tan(sp) \quad l_2 = 688.337$$

$$l := l_2 - l_1$$

$$l = 116.593$$



$$\max(\text{Gain}) = 5.025 \cdot 10^5$$

$$\text{Gain}_{2000} = 2.54 \cdot 10^5$$

**Biréfringence Walk-Off angle  $\rho$ :**

$$\rho := \text{atan} \left[ \left( \frac{n_{po}}{n_{pe}} \right)^2 \cdot \tan(\theta_c) \right] - \theta_c$$

$$\rho = 3.287 \cdot \text{deg}$$

$$\rho_1 := \text{atan} \left[ \frac{n_p(\theta_c)^2}{2} \cdot \left( \frac{1}{n_{pe}^2} - \frac{1}{n_{po}^2} \right) \cdot \sin(2 \cdot \theta_c) \right]$$

$$\rho_1 = 3.287 \cdot \text{deg}$$

**Real angle between the pump and signal beam:**

$$\alpha := \rho - \alpha_1$$

$$\alpha = 0.947 \cdot \text{deg}$$

+

**Deviation of the signal beam compared with the pump beam:**

-----  
**Defining angles and lengths :**

$$s := \theta - \theta_c + \alpha_1 \quad s = 4.669 \cdot \text{deg}$$

$$l_1 := \frac{L}{2} \cdot \tan(s) \quad l_1 = 571.743$$

$$sp := \theta - \theta_c + \rho \quad sp = 5.616 \cdot \text{deg}$$

$$l_2 := \frac{L}{2} \cdot \tan(sp) \quad l_2 = 688.337$$

$$l := l_2 - l_1$$

$$l = 116.593$$

**Defining of the Pump beam Diameter so that the Signal beam stay within the 80% intensity area of the Pump beam :**

$$w_p := 0.085$$

$$w_s := 0.05$$

$$I_p(r) := e^{-\frac{2 \cdot (r)^2}{w_p^2}}$$

$$I_s(r) := e^{-\frac{2 \cdot (r - 1 \cdot 10^{-4})^2}{w_s^2}}$$

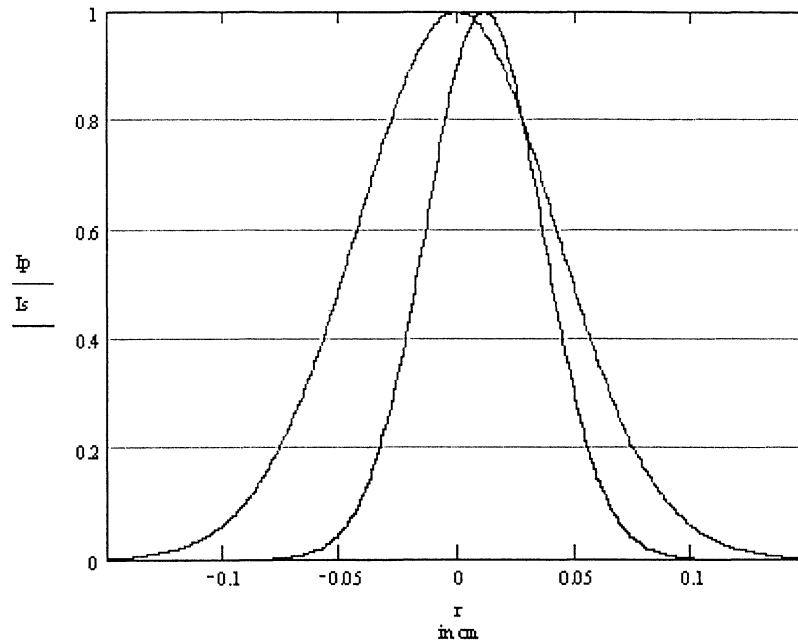
```
r(rmin, rmax, rstep) :=
| count ← 0
| for rr ∈ rmin, rmin + rstep .. rmax
|   | v_count ← rr
|   | count ← count + 1
| v
```

```
I_p(rmin, rmax, rstep) :=
| count ← 0
| for rr ∈ rmin, rmin + rstep .. rmax
|   | v_count ← I_p(rr)
|   | count ← count + 1
| v
```

```
I_s(rmin, rmax, rstep) :=
| count ← 0
| for rr ∈ rmin, rmin + rstep .. rmax
|   | v_count ← I_s(rr)
|   | count ← count + 1
| v
```

$$I_p := I_p(-0.15, 0.15, 0.0001) \quad I_s := I_s(-0.15, 0.15, 0.0001)$$

$$r := r(-0.15, 0.15, 0.0001)$$



**Pump Depletion (the pump beam has a Gaussian profile):**

**Calculation of the total energy of the Pump beam :**

-----  
 $I_{\text{peak}} := 0.545$

$\tau := 8$

$$I_{\text{total}} := 2 \cdot \int_0^{0.15} \int_0^{0.15} I_{\text{peak}} \cdot e^{-\frac{2 \cdot (x+y)^2}{w_p^2}} dx dy \quad I_{\text{total}} = 1.968 \cdot 10^{-3}$$

$E_p := I_{\text{total}} \cdot \tau$

$E_p = 0.016$

Calculation of the energy of the Output Signal beam :

$$E_{\text{input}} := 4 \cdot 10^{-9} \quad G := 10000$$

$$E_s := E_{\text{input}} \cdot G \quad E_s = 4 \cdot 10^{-5}$$

Calculation of the Pump Depletion :

$$\text{Depletion} := \frac{E_s}{E_p} \quad \text{Depletion} = 0.254 \%$$

Pump Depletion (the pump beam has a Top-Hat profile):

$$\mu\text{m} := 0.001 \text{ mm}$$

$$f := 770 \text{ cm} \quad a := 2.5 \text{ mm} \quad \lambda_p := 0.532 \mu\text{m} \quad I_0 := 4.36 \frac{\text{J}}{\text{cm}^2}$$

$$I(\rho) := \left[ 2 \cdot \frac{J_1 \left( \frac{2 \cdot \pi \cdot a \cdot \rho \cdot \mu\text{m}}{\lambda_p \cdot f} \right)}{\frac{2 \cdot \pi \cdot a \cdot \rho \cdot \mu\text{m}}{\lambda_p \cdot f}} \right]^2$$

$$yy := 500$$

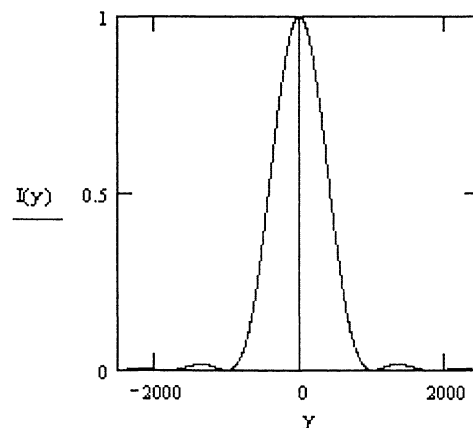
Given

$$I(yy) = 0.5 \quad \text{ysearch} := \text{Find}(yy)$$

$$\text{ysearch} = 421.517$$

$$w := 2 \cdot \text{ysearch} \quad w = 843.034$$

$$E(\rho) := 2 \cdot \int_0^{\frac{2 \cdot \pi \cdot a \cdot \rho}{\lambda_p \cdot f}} \left( \frac{J_1(x)}{x} \right)^2 dx$$



$$Et := E \left( \frac{0.61 \cdot \lambda_p \cdot f}{a} \right) \cdot \frac{\lambda_p^2 \cdot f^2}{\pi \cdot a^2} \cdot 10$$

$$Et = 0.031 \cdot \text{kg} \cdot \text{m}^2 \cdot \text{s}^{-2}$$

Calculation of the Pump Depletion :

$$Es := 4 \cdot 10^{-5} \text{ kg} \cdot \text{m}^2 \cdot \text{s}^{-2}$$

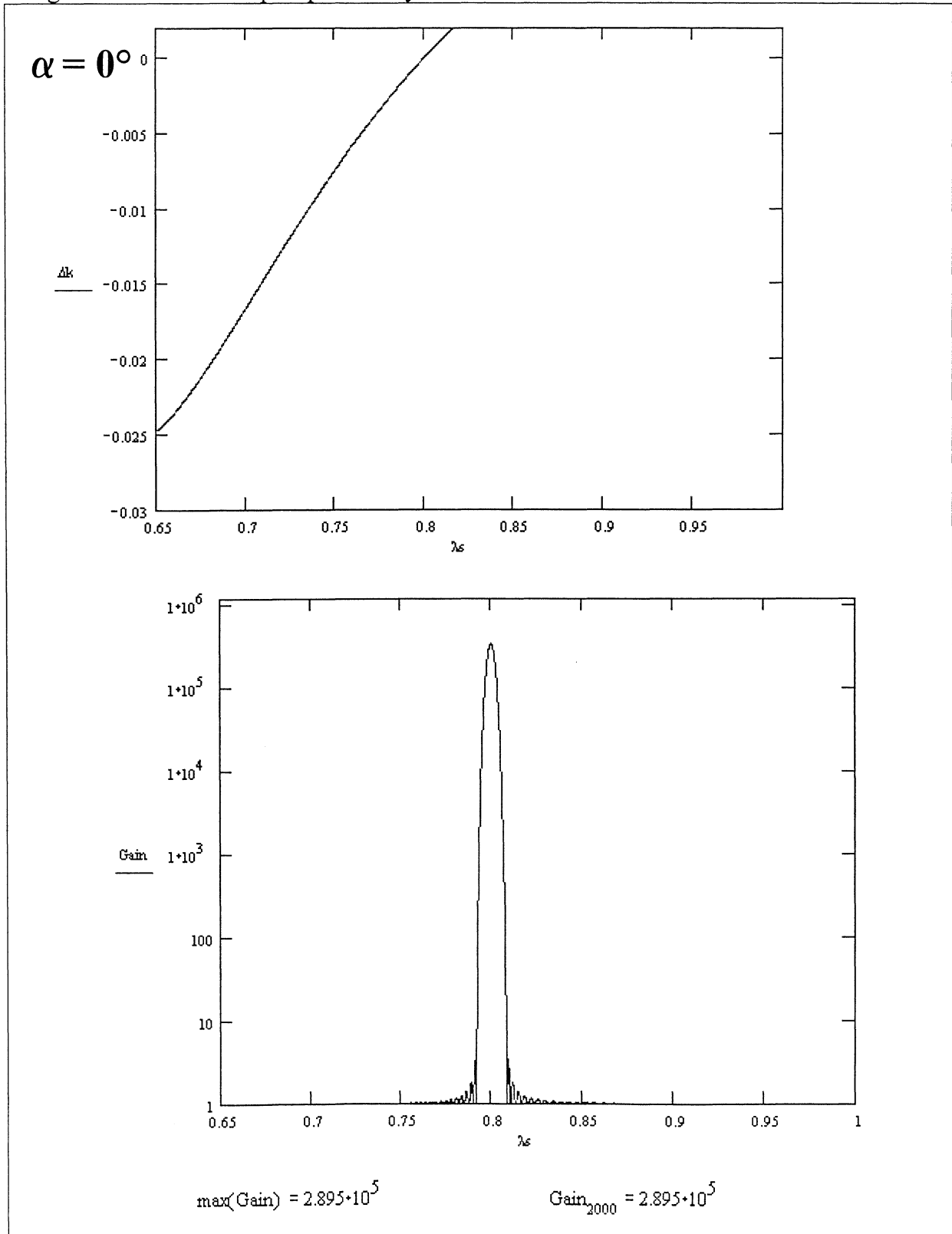
---

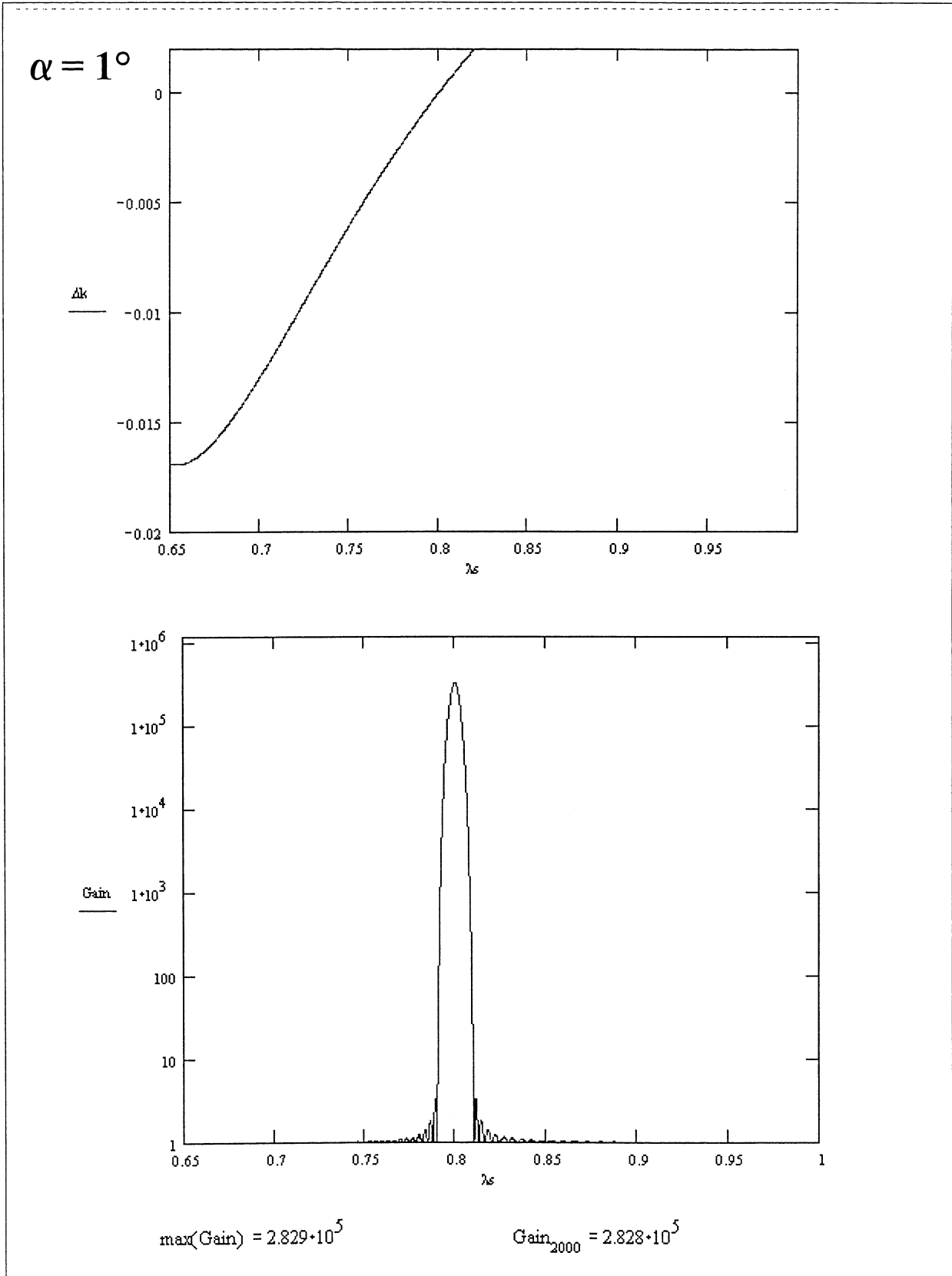
$$\text{Depletion} := \frac{Es}{Et}$$

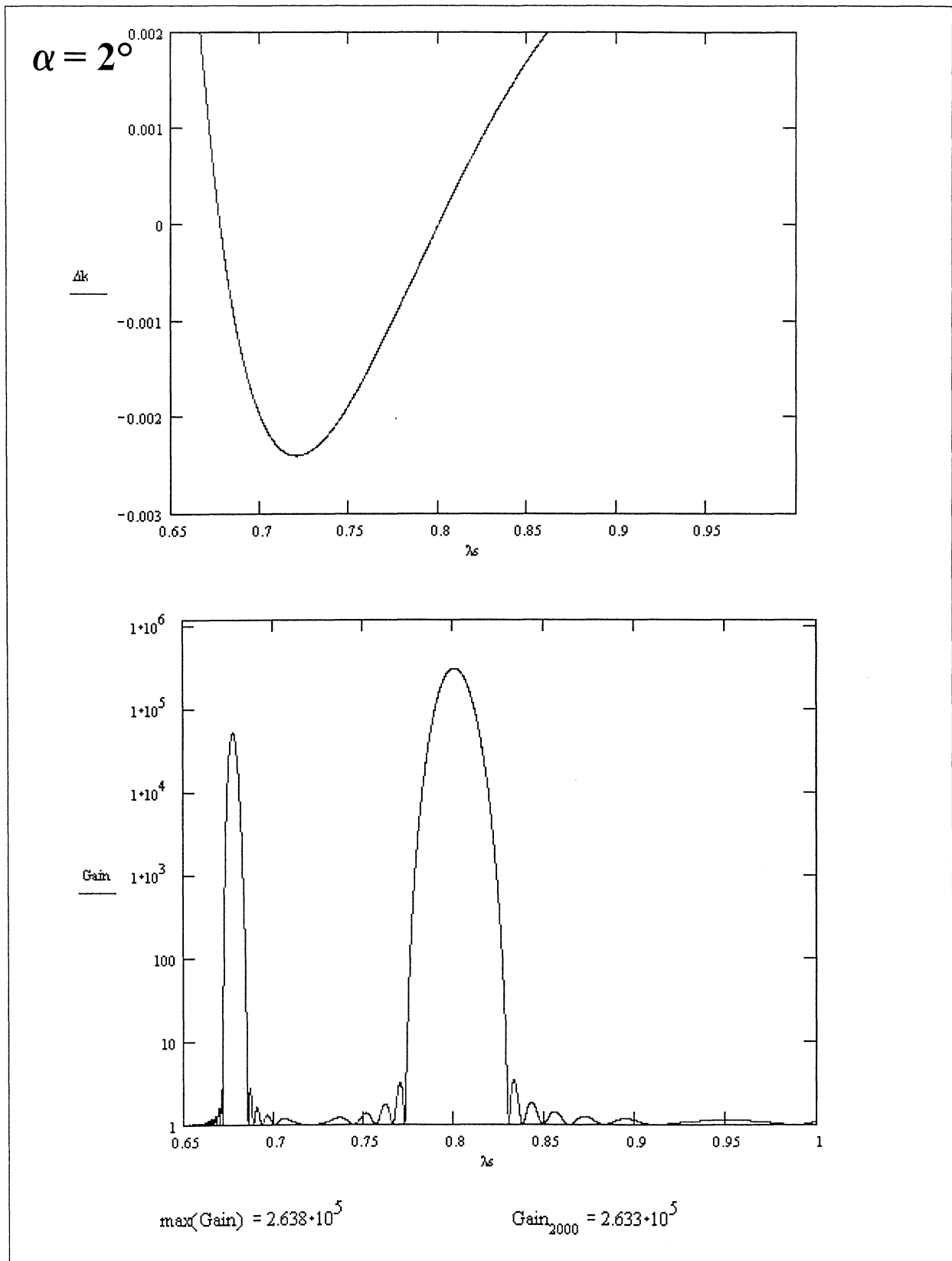
$$\text{Depletion} = 0.13 \%$$

## Annexe II

This annexe shows the shape of the phase mismatch and the gain curve for several values of the non-collinearity angle varying from 0 to 3 degrees with a interaction length of 14 mm and a pump intensity of  $1\text{GW}/\text{cm}^2$ .

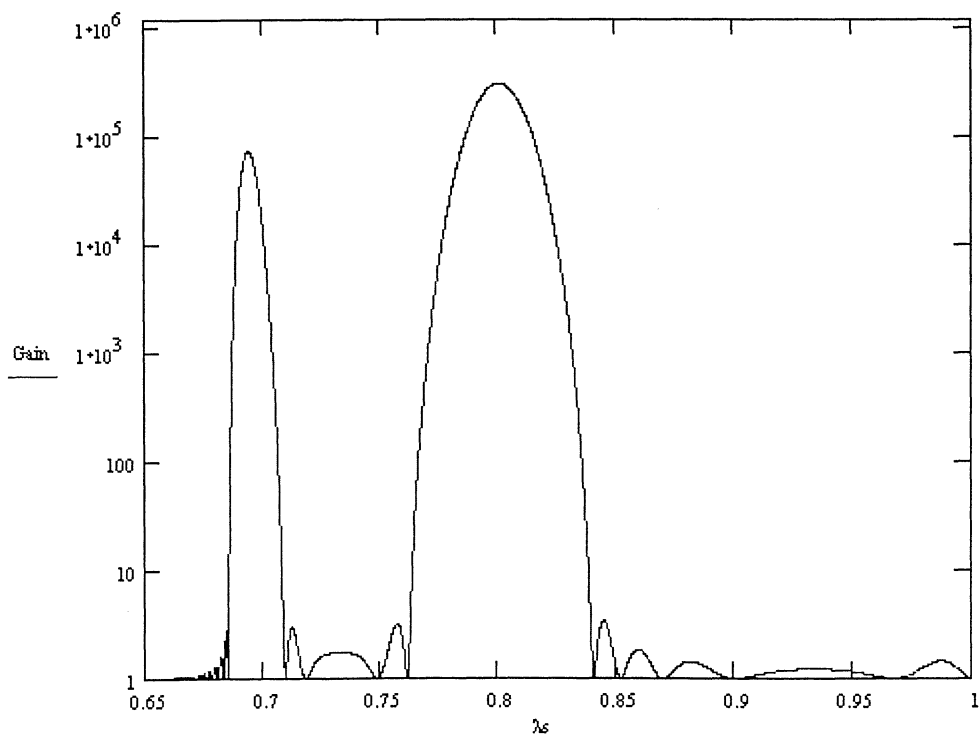
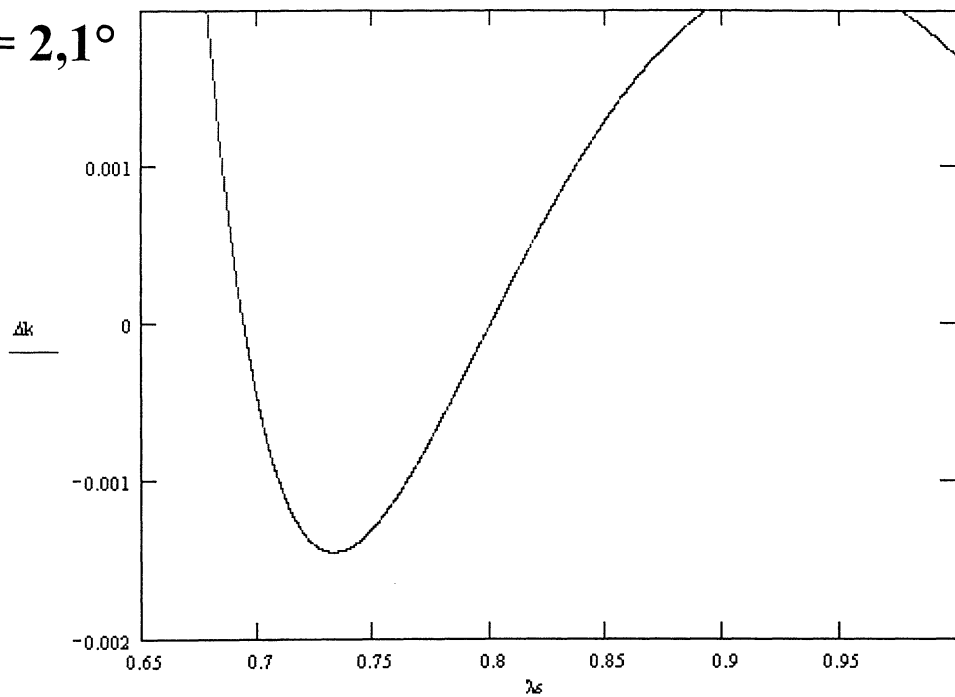






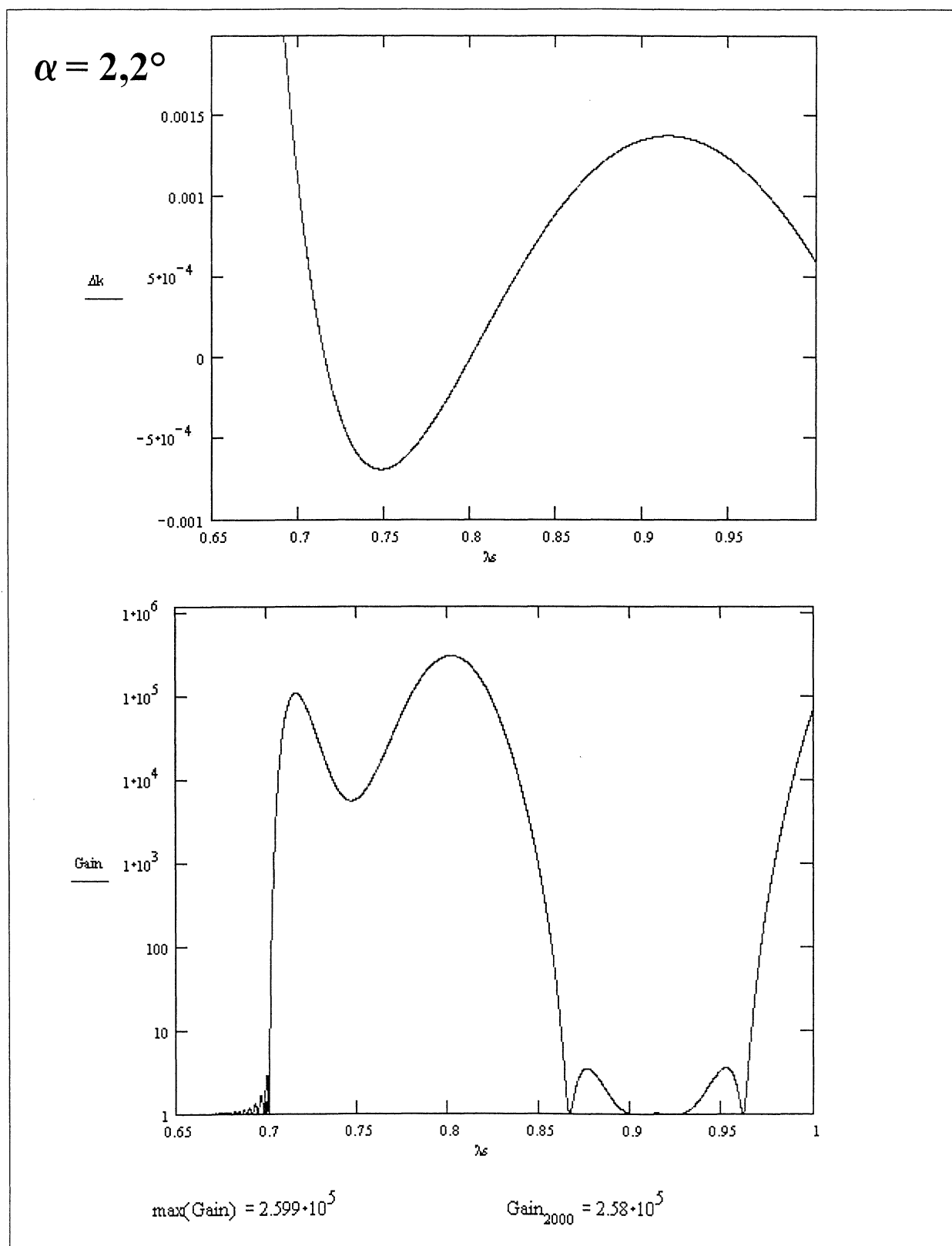


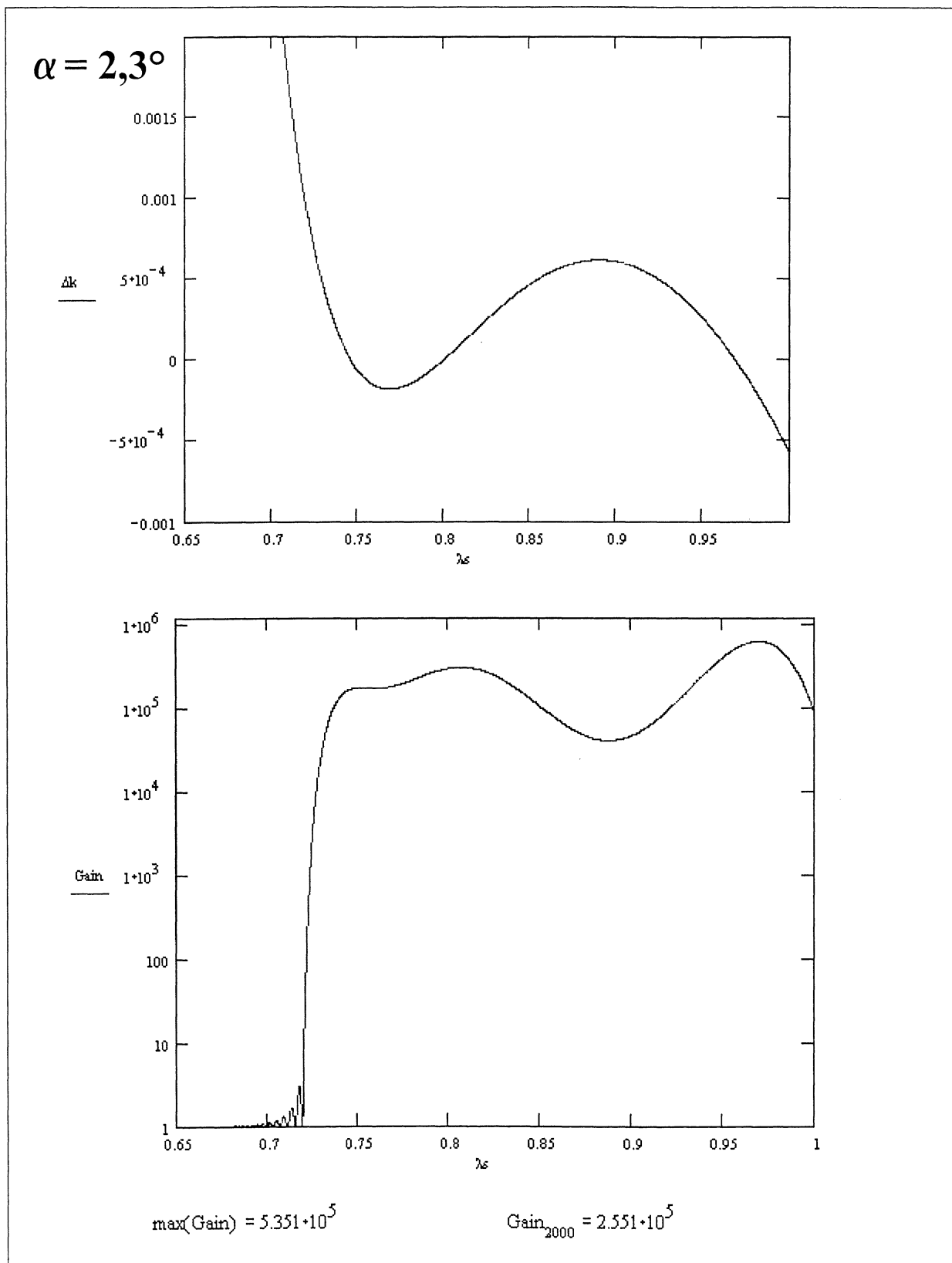
$\alpha = 2,1^\circ$

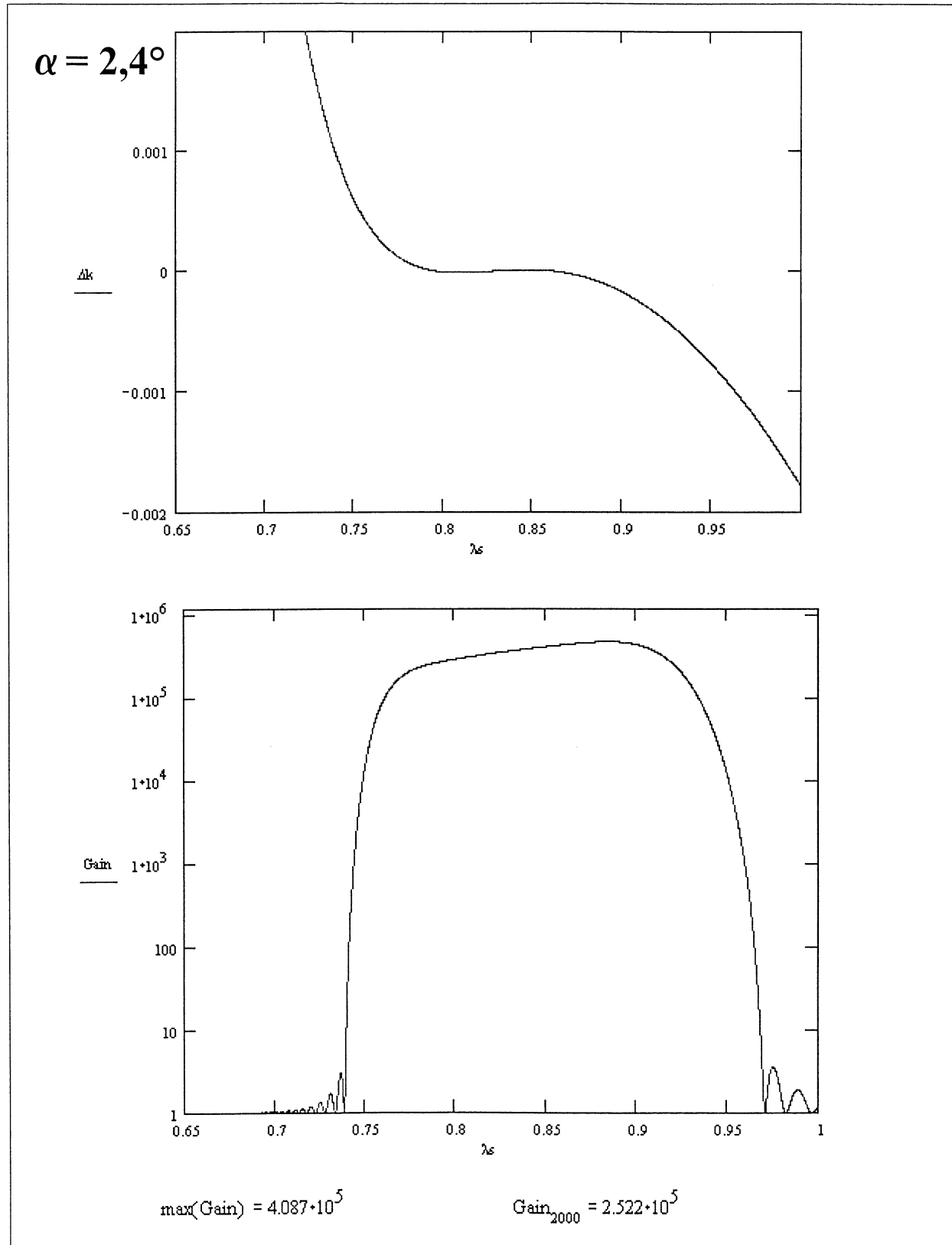


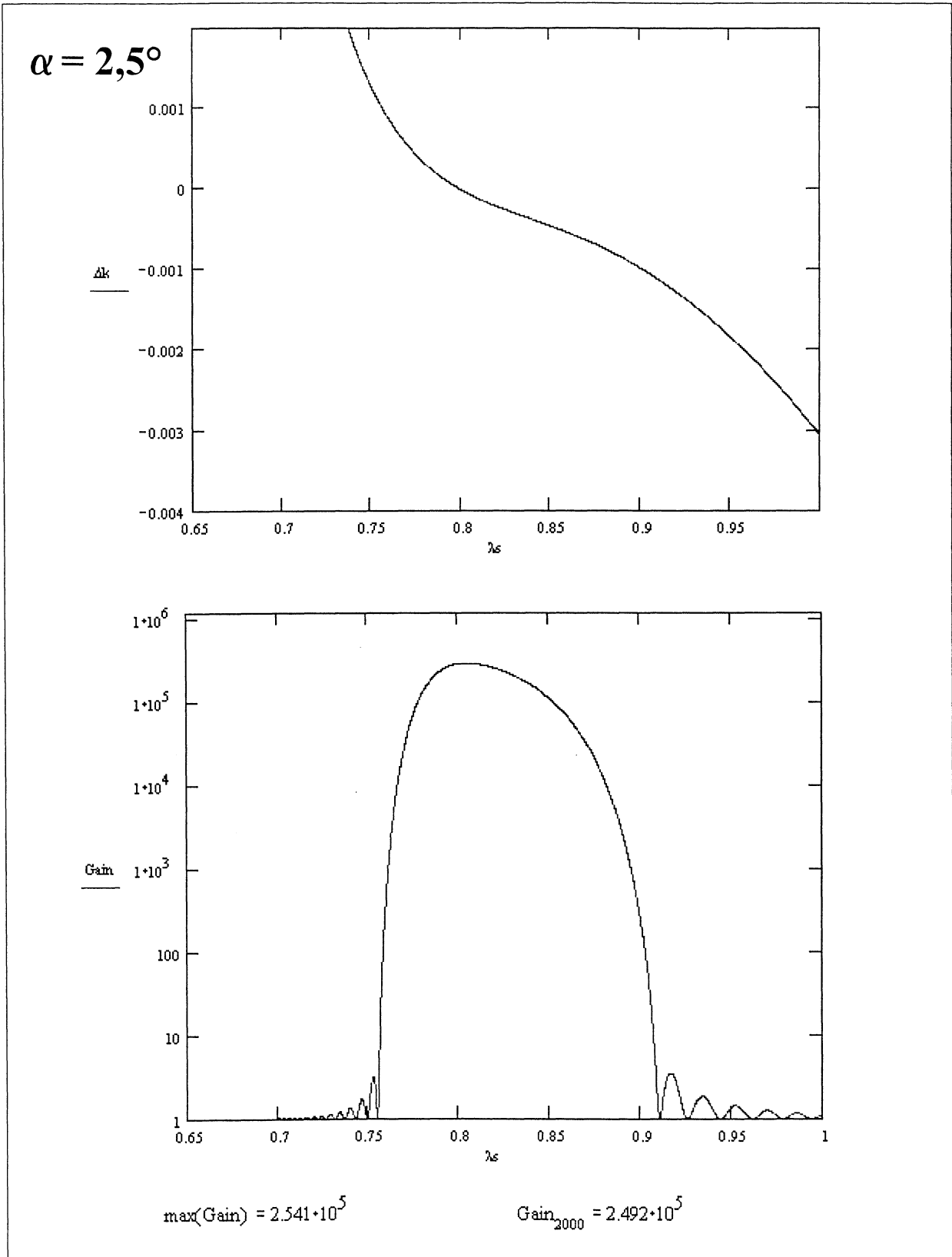
$\max(\text{Gain}) = 2.615 \cdot 10^5$

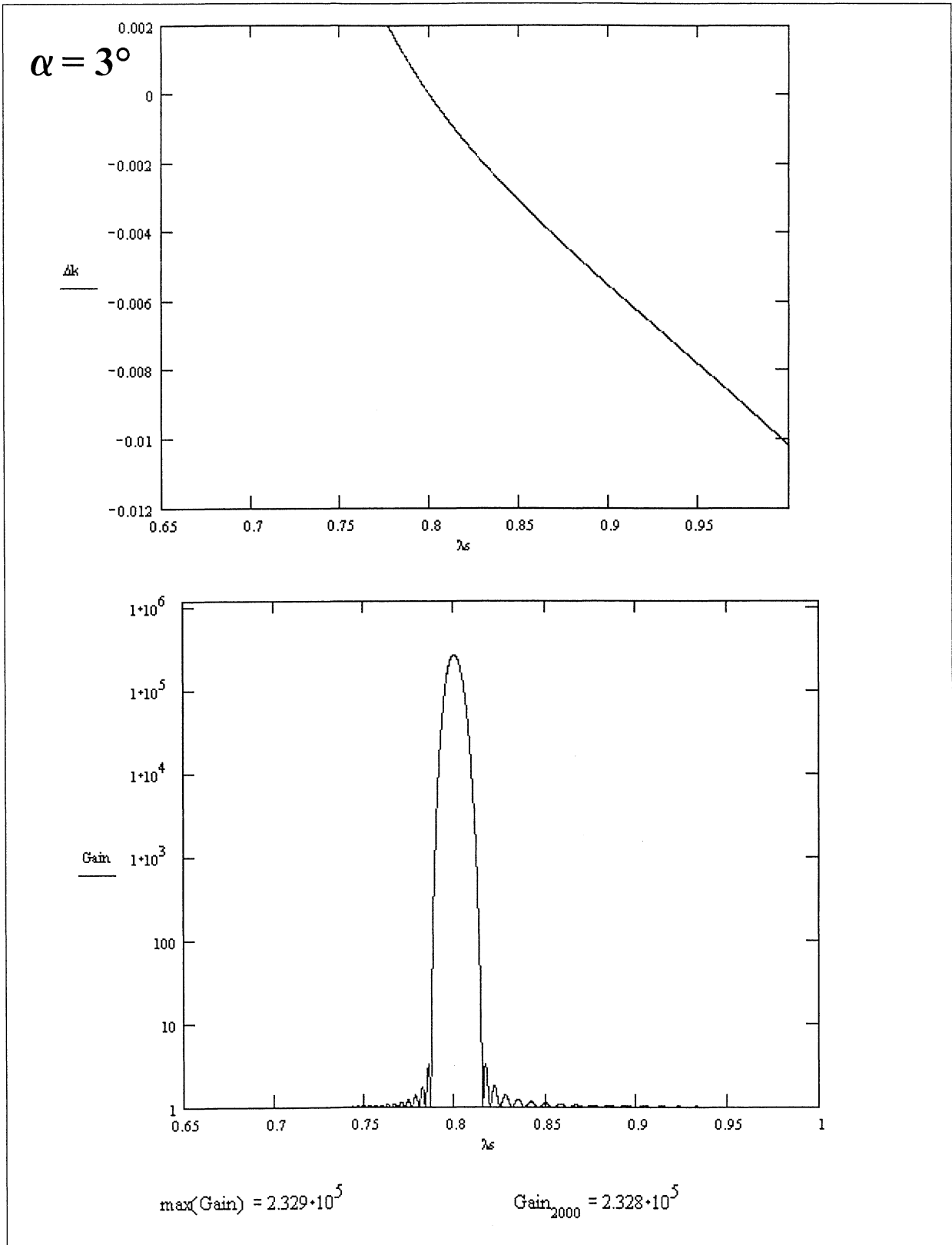
$\text{Gain}_{2000} = 2.607 \cdot 10^5$











# Experimental Setup

